Towards a global network of rotation sensors: ring laser data acquisition and online visualization

Jan N. Hautmann

March 2008

Geophysics

Department of Earth and Environmental Sciences

Ludwig-Maximilians-University Munich

For my parents and grandparents

Prof. Dr. Heiner Igel
Department of Earth and Environmental Sciences
Section Geophysics
Ludwig-Maximilians-University Munich

Prof. Dr. Ulrich Schreiber
Forschungseinrichtung Satellitengeodäsie
Technical University of Munich
Fundamentalstation Wettzell, Kötzding, Germany

Dr. Joachim Wassermann
Department of Earth and Environmental Sciences
Section Geophysics
Geophysical Observatory Fürstenfeldbruck
Ludwig-Maximilians-University Munich

Prof. Dr. Frank Vernon
Scripps Institution of Oceanography
University of California, San Diego

Acknowledgements

First of all, I want to thank my supervisor Prof. Heiner Igel for giving me the opportunity of participating in the ring laser project, which opened up the chance to experience theoretical and applied science in an international working group.

Special thanks are dedicated to Prof. Ulrich Schreiber who guided me during my stays at the Physics Department at the University of Christchurch and the Piñon Flat observatory in the US. He explained everything there is to know about ring laser physics and answered uncountable questions.

Dr. Joachim Wassermann shared his great technical experience, his knowledge in data processing and analysis with me, helping this thesis to become what it is.

Robert Barsch of the seismology group at the LMU Munich gave me insight to his extensive computer and programming knowledge, offering me support and guidance throughout my thesis.

Furthermore, I would like to thank the following colleagues and friends: Prof. Frank Vernon from the SCRIPPS Institute of Oceanography, Dr. Alexander Velikoseltsev and Dr. Alexander Neidhardt from the Fundamentalstation Wettzell, Dr. Wiwit Suryanto, Susanne Lehndorfer, Moritz Beyreuther and Gilbert Brietzke from the Seismology group of the LMU Munich.

The dedication and support I experienced from my family, my parents and grandparents during my academic studies was overwhelming. Thank you for everything.

Abstract

Rotational motions caused by earthquake waves have become a new observable for seismologists in the last decade. Employing ring laser technology provides the possibility to measure these rotations over a broad band of frequencies and magnitudes. In order to be useful for scientists, the long term data recorded by these instruments has to be available in a standard data format. The aim of this thesis is to create an online platform, presenting the data from three ring laser observatories, based in: Wettzell (Germany), Christchurch (New Zealand) and Piñon Flat (USA).

Due to the dissimilar data acquisition and storage techniques employed at these facilities, three main steps were required: establishing the continuous dataflow from the stations, converting the acquired data into a standard format (miniSeed) and online visualization of the stored data. In order to overcome the technical differences and to improve the performance of the systems, several hardware and software adjustments were carried out at the stations in Wettzell and Piñon Flat.

The resulting data is presented on the website of the International Working Group on Rotational Seismology (IWGoRS): http://www.rotational-seismology.org/data. Based on the fact that only the Piñon Flat station was originally designed to be used in broadband seismology, different transfer and visualization approaches for the laboratories had to be applied. The near real time data transfer from the station in Wettzell is realized using the SeedLink software, which allows for the storage of the raw data in the miniSeed format. A similar approach is applied for the observatory in Christchurch. The recorded data from Piñon Flat is downloaded and converted once every 24 hours, by employing a number of python- and shell-coded scripts developed during this thesis. We were able to record a number of Mag 6 and higher earthquakes since the establishment of the near real time data streams. However, a unified hardware and software solution concerning the data acquisition, transport and storage is desirable for future ring laser laboratories, easing the further study of rotational motions in seismology.

Abstract

Contents

Contents

Chapter 1.

Introduction

1.1. Measuring rotational motions in seismology

In seismology the observation of earthquake induced ground motion and the processing and interpretation of the recorded data are of great interest. Over the last decades translational ground motions (displacement, velocity or acceleration) have been recorded on a large scale and offered a better understanding of the interior of planet earth and earthquake rupture processes. The most important instruments for those observations are standard three-axis seismometers, providing the possibility to measure three components of translation along orthogonal axes. However, to fully describe the ground motion at a given point, six components of strain and three components of rotation need to be measured in addition to translations.

Though theoreticians pointed out the importance of rotational motions, these components were disregarded in the past for two reasons: the signal's amplitudes were thought to be too small to be measured (Bouchon and Aki, 1982) and no instrument featured the required sensitivity (Aki and Richards, 2002) to be useful for seismology. In the recent past several studies showed the possibility of measuring these missing components with state of the art technology, like: seismometer arrays (Spudich et al., 1995; Huang, 2003; Suryanto et al., 2006), parallel seismographs (Solarz et al., 2004; Teisseyre et al., 2003), solid state sensors (Nigbor, 1994; Takeo, 1998) and instruments employing the sagnac effect for measuring rotational motions - fibre optic gyroscopes and ring laser gyroscopes (Schreiber et al., 2005, 2006; Igel et al., 2005; Suryanto et al., 2006).

All of the sensors mentioned above provide the possibility of extracting information on the rotational component of earthquake waves. Although the preconditions for near field measurements are fulfilled by e.g. fibre optic technology or solid state sensors (Nigbor, 1994; Takeo, 1998), after the thorough analysis of ring laser measurements, the demands of broadband seismology, with expected angular velocities of $10^{-14}rad/s \leq \Omega_s \leq 10^{-4}rad/s$ (Schreiber et al., 2005) can only be achieved by ring laser gyroscopes (Cochard et al., 2006; Igel et al., 2007) to the best of our knowledge. Originally used for the highly precise measurements of variations in earths rotation rate (Stedman et al., 1995; Stedman, 2001), a ring laser gyroscope was used to determine the rotational component of earthquake waves in the late 1990s for the first time (McLeod et al., 1998; Pancha et al., 2000). A very good correlation of transverse acceleration derived from standard seismometer recordings and rotation rate obtained with ring laser gyroscopes was reported (Igel et al., 2005), verifying the measured quantity. The consistency in phase and amplitude was observed for a broad band of distances and magnitudes (Igel et al., 2007).

Even though more research has to be conducted in the area of rotational seismology, several studies already pointed out potential benefits for science. Point measurements of horizontal phase velocities (Igel et al., 2007), estimations of their direction of propagation and the specification of exact SH-wave arrival times (using a horizontally mounted gyroscope) are feasible. Standard seismometers' recordings are influenced by the rotational component of earthquake waves and surface tilt. As ring laser gyroscopes are in principle insensitive to translations, these instruments can easily be employed for data correction. The rotational component is also expected to provide additional information on earthquake rupture processes and for earthquake engineers. In the mid 1980s a pioneering theoretical study conducted by Bouchon and Aki (1982) presented earthquake scenarios showing relatively small rotation angles. As there is a strong mathematical connection between rotations and phase velocities, the rotation rates increase significantly with decreasing phase velocities (Cochard et al., 2006). Therefore, not only in long structures like bridges, pipelines or large edifices, significant damage can be expected arising from the rotational component, which is unaccounted for in civil engineering so far.

At the present stage, there are four ring laser observatories worldwide, conducting long term observations of rotational components induced by earthquakes. As the technology improved significantly in the last decade, ring lasers are now applicable as standard instruments for seismological measurements. However, an instrument detecting all

three components of rotation is still to be constructed. Momentarily, portable instruments are being developed, aiming at recording three components of translation and the collocated three components of rotation at volcanoes or in aftershock regions.

1.2. Motivation

To the present day, scientists are still struggling to fully explain the driving mechanisms triggering earthquakes all over our planet. The damage caused by these events is often clearly visible and not only of economic nature. A possible way to confront these scenarios is trying to completely understand the driving forces leading to rupture processes and the generation of earthquake waves. Seismology offers the possibility to study the forces leading to the destructive motions of earth's surface. Seismologists mainly focused on translational ground motions, as suitable instruments to measure this component of motion benefited from the technological evolution in the 19th century. This development led to the possibility of observing translational motions caused by earthquake waves worldwide, 24 hours on 365 days a year. Seismometer and computer networks are employed to create a very complex system of data transport, storage and access.

Rotational motions however were neglected until the mid 1990s, when ring laser technology offered the chance of detecting rotational motions caused by near field and teleseismic events. These instruments, originally developed for geodetic purposes, soon turned out to be very useful for seismology. The insensitivity towards translational motions and a very high resolution enabled scientists to conduct the most accurate observations of rotation rates so far.

After a long development, there are four major ring laser observatories worldwide today measuring rotational ground motions over a broad range of magnitudes and frequencies:

- Wettzell, Germany
- Christchurch, New Zealand
- Piñon Flat, USA
- Arkansas, USA.

At all of these laboratories, one or more ring laser gyroscopes are detecting rotational motions around a vertical axis. However, the Christchurch observatory offers the unique opportunity of measuring rotations around a horizontal axis.

Due to the novelty of this technology, in comparison to the advanced seismometer

networks, a lack in standardisation of the following aspects has to be noted in ring laser seismology:

- data recording
- data storage
- naming convention
- data access
- data transport
- data online visualization
- data (pre-)processing.

As the gyroscope at the Piñon Flat observatory is the only instrument specially designed for seismological applications, it is a technical challenge to introduce standard procedures like the ones mentioned above for all laboratories. In this thesis the main focus is laid on data transfer and online visualization, establishing a standard storage data format (miniSeed) and a standard data transfer for the stations in Wettzell and Christchurch. Combining the existing systems to a network of rotation sensors, enabling online visualization and providing the chance of easily enhancing this network with a growing number of ring laser laboratories is a very challenging task with ever changing requirements.

1.3. Thesis outline

The developments carried out in the field of ring laser technology, data transfer, data conversion and online visualization is presented in detail in this thesis. Each chapter is dedicated to one aspect of theory or application:

- The first chapter of this thesis gives an introduction to the topic of rotation measurements in seismology and holds the motivation for the thesis.

- The second chapter explains the mathematics behind the rotational motions and gives a description of the different approaches on measuring rotational motions in seismology.

- In the third chapter the instrumentation of the observatories in Wettzell (Germany), Christchurch (New Zealand) and Piñon Flat (USA) is characterized in detail.

- Chapter four explains the different data transfer and data conversion applications used to create a standard data portal.

- In chapter five, a summary, conclusions and an outlook on the future of instruments measuring rotational motions in seismology is presented.

Three attached appendices present the codes developed during this thesis in Appendix A, an overview of the conventions for GSE-files in Appendix B and Appendix C.

Chapter 2.

Theory

2.1. Rotational motions

Earthquake induced ground motions have been recorded and monitored by seismologists for more than 100 years. The instruments of choice were, and still are, three-axis seismometers and strain meters. A major goal of geophysics and civil engineering is to describe the motion of a certain point at the earth's surface completely, by determining the necessary variables: three components of translation, six components of strain and three components of rotation. A suitable equipment to record rotation data was missing up to the mid 1990s. At teleseismic distances the rotational motions measured at the stations are created by surface waves primarily. Other effects resulting in rotational motions will be mentioned later in this chapter.

The rotation at any point on the earth's surface is proportional to the curl of a vector field, which can be used to describe seismic waves. According to Aki and Richards (2002), the displacement from one point $\mathbf{x}$ to the next point - employing classical elasticity and assuming infinitesimal deformations (Cochard et al., 2006) $\boldsymbol{x} + \delta\boldsymbol{x}$ - is given by:

$$
\begin{aligned}
\mathbf{u}(\mathbf{x} + \delta\mathbf{x}) &= \mathbf{u}(\mathbf{x}) + G\delta\mathbf{x} \\
&= \mathbf{u}(\mathbf{x}) + \epsilon\delta\mathbf{x} + \Omega\delta\mathbf{x} \\
&= \mathbf{u}(\mathbf{x}) + \epsilon\delta\mathbf{x} + \omega \times \delta\mathbf{x}
\end{aligned}
\tag{2.1}
$$

with second order tensors: gradient of deformation G, strain ϵ and rotation Ω. The necessity of having three components of translation, six components of strain, and three components of rotation is illustrated by the (pseudo-)vector

$$
\omega = \frac{1}{2} \bigtriangledown \times \mathbf{u},
\tag{2.2}
$$

giving the angle of rigid body rotation with $\bigtriangledown$ representing the nabla operator.

2.1.1. A double couple point source

A double couple point shear dislocation is the best model for the description of earthquake sources. Assuming such a double couple source in an infinite, homogeneous and isotropic medium, Aki and Richards (2002) define the time dependent displacement *u(x,t)* by

$$
\begin{aligned}
\mathbf{u}(\mathbf{x}, t) = & \frac{1}{4\pi\rho} \mathbf{A}^N \frac{1}{r^4} \int_{\frac{r}{\alpha}}^{\frac{r}{\beta}} \tau M_0(t - \tau) d\tau \\
& + \frac{1}{4\pi\rho\alpha^2} \mathbf{A}^{IP} \frac{1}{r^2} M_0(t - \frac{r}{\alpha}) \\
& + \frac{1}{4\pi\rho\beta^2} \mathbf{A}^{IS} \frac{1}{r^2} M_0(t - \frac{r}{\beta}) \\
& + \frac{1}{4\pi\rho\alpha^3} \mathbf{A}^{FP} \frac{1}{r} \dot{M}_0(t - \frac{r}{\alpha}) \\
& + \frac{1}{4\pi\rho\alpha^3} \mathbf{A}^{IS} \frac{1}{r} \dot{M}_0(t - \frac{r}{\beta})
\end{aligned}
\tag{2.3}
$$

when the shear dislocation is in the (x_1, x_2) plane (see Aki and Richards 2002, page 79, figure 4.4) and the slip along x_1. Here $M_0(t)$ is the time dependent moment, the functions A and their superscripts define the radiation patterns for near field (N), intermediate (I) and far field (F) with (S) and (P) denoting the wave types. In order to calculate the rigid body rotation, equation 2.2 (page 7) is applied to equation 2.1 (page 7), resulting in:

$$
\begin{aligned}
\omega(\mathbf{x}, t) = & \frac{1}{2} \bigtriangledown \times \mathbf{u}(\mathbf{x}, t) \\
= & \frac{-\mathbf{A}^R}{8\pi\rho} [\frac{3}{\beta^2 r^3} M_0(t - \frac{r}{\beta}) + \frac{3}{\beta^3 r^2} \dot{M}_0(t - \frac{r}{\beta}) + \frac{3}{\beta^4 r} \ddot{M}_0(t - \frac{r}{\beta})]
\end{aligned}
\tag{2.4}
$$

(Cochard et al., 2006) with the radiation pattern of the three components of rotation given by

$$
\mathbf{A}^R = cos\Theta sin\Phi \hat{\boldsymbol{\Theta}} + \cos \Phi cos2\Theta \hat{\boldsymbol{\Phi}}.
\tag{2.5}
$$

The transverse far field radiation pattern $(\mathbf{A}^{FS})$ can be used for the calculation of $\mathbf{A}^R$:

$$
\bigtriangledown \times \mathbf{A}^{FS} = \frac{\mathbf{A}^R}{r}.
\tag{2.6}
$$

The divergence is calculated similarly as

$$\bigtriangledown \times \mathbf{u}(\mathbf{x}) = \frac{-\mathbf{A}^D}{4\pi\rho}[\frac{3}{\alpha^2 r^3}M_0(t - \frac{r}{\alpha} + \frac{3}{\alpha^3 r^2}\dot{M}_0(t - \frac{r}{\alpha} + \frac{3}{\alpha^4 r}\ddot{M}_0(t - \frac{r}{\alpha}] \qquad (2.7)$$

and the radiation pattern of the divergence is given by:

$$\mathbf{A}^D = cos\Phi sin2\Theta, \qquad (2.8)$$

connected to the radial far field radiation pattern by: $\mathbf{A}^{FP}$=$\mathbf{A}^D$r. As visible on rotational seismograms, rotations are zero at the P wave front (Cochard et al., 2006) and the first onset can be seen starting with the S wave arrival.

2.1.2. Rotation and tilt

At the free surface, assuming zero traction boundary condition, where 'the vertical component of traction is zero' (Suryanto, 2007), it is implied that $\sigma_{i3} = \sigma_{3i} = 0$. In an homogeneous and isotropic medium, the implementation of Hooke's law $\sigma_{ij} = \lambda\epsilon_{kk} + 2\mu\epsilon_{ij}$ results in

$$\begin{aligned}
\frac{\partial u_x}{\partial x_z} &= -\frac{\partial u_z}{\partial x_x}; \\
\frac{\partial u_y}{\partial x_z} &= -\frac{\partial u_z}{\partial x_y}; \\
\frac{\partial u_z}{\partial x_z} &= -\frac{\lambda}{\lambda + 2\mu}(\frac{\partial u_x}{\partial x_x} + (\frac{\partial u_y}{\partial x_y}),
\end{aligned} \qquad (2.9)$$

leading to

$$\omega_x = \frac{\partial u_z}{\partial x_y}; \omega_y = -(\frac{\partial u_z}{\partial x_x}). \qquad (2.10)$$

This reveals, that horizontal rotation at earth's surface is equal to tilt. It remains to be defined, which instruments - tiltmeters or rotation meters like ring laser gyroscopes - are better suited for measuring this component, as classical tiltmeters cannot differ between a change in the local gravity vector and a true rotational signal. In the last decade however, the benefit of ring laser technology, providing the means to obtain the vertical component of the vector of rotation, became obvious. In order to compare the translational signals recorded by seismometers to the rotational signal recorded by the gyroscopes, the seismometer's horizontal components are rotated into radial and transversal directions (Igel et al., 2005). The traces - generated by horizontally polarized love waves - are differentiated with respect to time in order to get transverse acceleration. Under the plane wave assumption, the displacement **u** of a horizontally

polarized wave is given as

$$\mathbf{u} = (0, u_y(t - \frac{x}{c}), 0), \tag{2.11}$$

with c being the horizontal phase velocity. In order to calculate the vector of rotation, the curl operator has to be applied

$$\frac{1}{2} \bigtriangledown \times \mathbf{u} = (0, 0, -\frac{1}{2c}\dot{u}_y(t - \frac{x}{c})) \tag{2.12}$$

from which the z-component of the rotation rate can be derived as

$$\Omega_z(x, t) = -\frac{1}{2c}\ddot{u}_y(t - \frac{x}{c}). \tag{2.13}$$

The similarity of equation 2.12 and equation 2.13 leads to the conclusion that under the given assumptions, the rotation rate and the transverse acceleration are equal in phase and

$$\frac{\ddot{u}(x, t)}{\Omega_z(x, t)} = -2c \tag{2.14}$$

displays the relationship of the amplitudes (Igel et al., 2005). Based on the theory, the next sections of this chapter show the principles of measurement and instrument types in detail.

2.2. Measuring rotational motions

Detecting and recording rotational ground motions caused by earthquake waves (and other effects) offers a new field with a broad band of possibilities not only for seismologists. As mentioned before, the characterization of the displacement at a certain point depends on translations, strain and rotations. At the beginning mainly driven by geodesists, a lot of effort has been put into the development of rotation sensors since the 1990ies, when scientists realized the capability of new technologies and instruments. A number of studies were conducted in order to observe the rotation rate using different approaches (Takeo and Ito, 1997; Nigbor, 1994; Solarz et al., 2004). These devices, their benefits and disadvantages, will be explained in detail in the section 'rotation sensors'.

Although the real benefit to science is still under investigation (Cochard et al., 2006), the recording of rotational motions might provide additional information on earthquake source processes, e.g. close to active faults as in Takeo and Ito (1997). The estimation of permanent displacement from seismic recordings, the determination of local horizontal phase velocities as described in Igel et al. (2005) and an exact determination of SH-wave arrival times is feasible using these new devices. Employing

a three-component rotation sensor will not only help to fully define the motion of a certain point induced by earthquake waves for the first time. It will also help earthquake engineers to extract information on structure stability and rotational effects on buildings.

The field of rotational seismology is very new and a lot of questions are still not answered. All aspects from data acquisition, transfer, and storage to (pre-)processing and visualization need to be discussed and brought to meet standard requirements. It remains to be evaluated which instrument, or even which technology (or technologies) is (are) best suited to record the desired factors. It is probable that due to the range of applications (e.g. strong motion or teleseismic) different approaches of the same technology will be implemented.

There is a general difference in acquiring ring laser data and seismometer data. The seismometer delivers a voltage signal, that is directly proportional to the ground velocity. The ground rotation however is detected indirectly, via obtaining a frequency. The usage of a 20 Hz sampling rate is typical in broadband seismology. According to the sampling theorem (Scherbaum, 1996), at this sampling rate the nyquist frequency is 10 Hz and therefore suitable for seismological applications.

2.2.1. Rotations in earth sciences and other disciplines

The exact estimation of rotational motions is interesting for science and likewise for commercial applications. A large number of technical devices apply some form of rotational motion sensors today. The transport sector, e.g. in aviation, nautics and submarine robotics relies on the three components of rotation as an integral part of state of the art navigation systems. These instruments, fibre optic gyroscopes with a cavity length of up to 32 cm are very reliable, relatively cheap to manufacture and have a resolution so far not useful in seismology.

Though it was known to geophysicists for the last decades, that rotations may play an important role, geodesy occupied the most sensitive instruments for detecting these motions. The determination of earth's rotation rate and its exact variations are measured in geodesy and astrometry using e.g. VLBI (Very Long Baseline Interferometry) since the 1970s. This technique requires two or more observatories recording the signals (microwave range) from distant radio sources, extracting information about the geometrical orientation of the rotating earth by interferometry.

Today ring laser technology provides the possibility of recording the variations with as little as one single station independently from local reference systems. Though primarily developed for the detection of earth's rotation rate and tides (Schreiber et al., 2003) this technology finds application in seismology, recording the rotational compo-

nent of earthquake waves today. The destruction of buildings and large structures due to the influence of earthquake waves is often their most visible effect. Civil engineers are concerned with the response of buildings and large structures, such as bridges and pipelines. Translational motions caused by surface waves with large amplitudes and a high content of energy are known to cause major damage. This is among other things one of the factors that led to the negligence of studies concerned with rotational motions. Today, civil engineers still await highly sensitive fibre optic gyroscopes to estimate the buildings' response functions by detecting the torsional motions. What kind of rotation sensors already find application in geophysical studies is explained in the next sections.

2.3. Rotational sensors

In the last two decades a number of rotational sensors became available for seismologists. Commercial sensors usually find application in near field studies, while the recording of teleseismic events is limited to technology specially designed for seismological applications. The most important of these are described in the next section.

2.3.1. Solid state sensors

This type of rotation sensor is inexpensive, easy to manufacture and can be very small (5mm), finding application in navigation systems, instruments in moving vehicles and as stabilization. The device consists of two quartz tuning forks - aligned along one axis pointing in opposite directions - and a GyroChip (Suryanto, 2007). The idea of a vibrating element detecting the rotational velocity based on the Coriolis principle is exploited by this technique. Employing a three-axis accelerometer and this sensor, Nigbor (1994) measured translational and rotational ground motions in Nevada for the first time. Takeo (1998) used a similar device for the detection of an earthquake swarm on the Izu peninsula in Japan. However it can be reported, that this technology is suitable only for large ground motions close to the source, which makes it unsuitable for broadband seismology.

2.3.2. Parallel seismograph

The TAPS system consists of *two antiparallel pendulum seismometers*, which are orientated oppositely around a common axis. This system was first shown by Moriya and

Marumo (1998), similar to the rotation-seismograph used by Teisseyre et al. (2003). The rotational component is calculated based on the recordings measured by the two seismometers. A number of seismic events were detected with this system in Poland and Italy, however, the bandwidth of limits the application to near field events as well. A comparison to other rotation meters has not yet been conducted.

2.3.3. Eentec R1

The R1 is a triaxial rotational velocity sensor. The measurement is based on an electrochemical (magnetohydrodynamic) principle. This device, developed by Eentec Inc., is relatively cheap and small (12cm x 12cm x 9cm). Up to the writing of this thesis, no intensive studies have been conducted pointing out the quality of this apparatus. Its response has recently been tested on a shaking table the results are yet to be published.

2.3.4. Seismometer array

Several studies derive the rotation rate from array measurements, employing three or more standard three-axis seismometers, have been conducted in the last 15 years, e.g. by Bodin et al. (1997); Huang (2003); Spudich and Fletcher (2008); Suryanto et al. (2006). Rotational motions can be estimated from the horizontal translation traces of array measurements by applying the curl-operator

$$
\begin{pmatrix} \omega_x \\ \omega_y \\ \omega_z \end{pmatrix} = \frac{1}{2} \bigtriangledown \times \overrightarrow{v} = \frac{1}{2} \begin{pmatrix} \partial_y v_z - \partial_z v_y \\ \partial_z v_x - \partial_x v_z \\ \partial_x v_y - \partial_y v_x \end{pmatrix}
\tag{2.15}
$$

to the seismic wave field $\overrightarrow{v}(x, y, z)$. The estimation of the derivatives is carried out by the subtraction of two recordings of ground displacement (velocities, acceleration) divided by there distance (Suryanto et al., 2006). The usage of standard seismometers offers the advantage of working with reliable and proven instruments. The study conducted by Suryanto et al. (2006) showed, that the array-derived rotation rate corresponds quite well to the directly obtained rotation rate (by the gyroscope) in the centre of the array. However, uncertainties in the seismometers location, noise and local soil condition effects can lead to erroneous data sets. Additionally the seismometers are sensitive to tilt on the surface, so with this method we derive rotational motions from instruments, whose recordings are contaminated by rotations.

2.3.5. Fibre optic gyroscopes

Fibre optic gyroscopes are passive sagnac interferometers that find a wide range of technical applications. The extraction of rotation rate is facilitated using the sagnac effect, which will be explained in detail in section 2.3.6 on page 15. Such a gyroscope consists of a fibre optic wire, a light source and a detection unit. No moving mechanical parts are involved in the rotation rate determination process. The gyroscopes' light beam path is defined by the fibre optic wire, allowing a very large enclosed area in a small chassis, as the wire can have a high number of windings (e.g. around the plate of Zerodur®[1] in Wettzell 2007, see figure 3.3).

According to formula 2.17 on page 16, the instruments' resolution increases with higher cavity length. This however is restricted due to thermal susceptibility of the fibre optic wire and nonreciprocity effects that eliminate the advantages of the larger scaling factor. The rotation rate is obtained as a phase difference measurement. This phase difference is proportional to the rotation rate, given by Velikoseltsev and Schreiber (2005) as

$$\triangle \varphi = \frac{8\pi \cdot N \cdot S_c}{\lambda \cdot c} = \frac{2\pi \cdot L \cdot D}{\lambda \cdot c} \cdot \Omega, \tag{2.16}$$

with

- N: number of windings of the fibre optic coil
- S_c: average area of the coil
- L: total length of the optic fibre
- D: mean diameter of the coil.

A very high sensitivity can theoretically be realized with stationary FOGs but applications in the area of re-deployable instruments are more likely. Portable FOG-stations could house a three axis seismometer and three fibre optic gyros, detecting rotational motions along perpendicular axes. An application tested momentarily serves civil engineers in monitoring structure response due to effects like earthquake waves or wind.

2.3.6. Ring laser gyroscopes

To the best of our knowledge, the most accurate way of measuring rotational motions caused by earthquakes and other effects, is through the application of ring laser technology. The measurement principle of this device is based on the sagnac effect. It offers the possibility to record rotations over a broad band of distances, frequencies and magnitudes (Igel et al., 2007). Originally developed for geodetic purposes, this technique

---

[1]Zerodur® is a glass ceramic with a very low coefficient of thermal expansion between 0.01 and 0.02·10⁻⁶ 1/K.

provides long term running stability and a very high resolution - needed for detecting even weak teleseismic events. According to the sagnac formula (see 2.17, page 16), the instrument is insensitive to translational motions and is therefore obtaining the 'true', unpolluted rotation signal. A correction of the recorded data using tilt measurements does not seem necessary (Dinh Pham, personal communication).

Due to the gyroscopes exceptional high sensitivity, additionally to rotational motions caused by earthquake waves, a whole number of effects can be seen in long term ring laser data, like

- earth's rotation rate,
- variation of earth's rotation rate,
- earth tides,
- mountaintalk (atmospheric effects on mountains), and
- free oscillations of the earth,

presupposing a constant level of ambient influences. The requirements for ring laser operation, the principles of the sagnac effect and the technical realization of these active interferometers is explained in the next subsection.

Principle of ring laser operation based on the sagnac effect

In 1913 the French physicist G. Sagnac performed the first ring interferometry experiment. Thereby he detected a phase-shift between two coherent light beams travelling on the same rectangular light path - one clockwise and one counterclockwise - when the apparatus was rotated. This phase-shift is what we refer to as 'sagnac effect' today. Thirteen years later A. Michelson and H. Gale instantiated an interferometer with an effective perimeter of 1.9 km, which allowed them to measure earth's rotation with an accuracy of 2%. These experiments and the resulting conclusions have become the basis for a technology used in various commercial devices as well as the gyroscopes discussed here.

A modern ring laser gyroscope uses the same principle for the detection of rotational motions as those interferometers: the sagnac effect. Inside the instrument two independent laser beams travel on the same light path, defined by mirrors, in opposite directions (see figure 2.1 on page 17). At one of the corners, the two counterpropagating laser beams, are superimposed (see subsection 2.3.6, page 18). The resulting (beat) frequency corresponds to earth's rotation rate, depending on the size and latitude of the instrument. A precondition for ring laser operation is an integral number of wavelengths for both directions of propagation. When the system is rotating with respect to inertial space, the result is a slight change in effective cavity length for the

co- and counterrotating laser beams. Therefore the detected beat frequency changes, as the laser beam frequencies increase and decrease respectively, proportional to the rate of rotation. The sagnac equation

$$\delta f = \frac{4A}{\lambda P}\mathbf{n} \cdot \mathbf{\Omega} \tag{2.17}$$

shows the relationship between the velocity of rotation $\mathbf{\Omega}$ measured around the surface normal $\mathbf{n}$. A is the effective area, λ the wavelength of the laser light and P the perimeter. Although ring laser gyroscopes are insensitive to translational motions, equation 2.17 shows, that the beat frequency δf can be influenced by variations in the rotation rate $\mathbf{\Omega}$, by variations of the scaling factor $(\frac{4A}{\lambda P})$ and due to changes in orientation of $\mathbf{n}$ Changes in the scaling factor can be eliminated by an extremely rigid design of the ring laser cavity. Special focus must be laid on the horizontal component of rotations (corresponding to tilt at the free surface), causing a very small signature in the horizontal component of rotation, as reported by Schreiber et al. (2005, 2006).

In order to verify the measured quantities, the rotational motions are compared to translations, measured by a standard seismometer, as explained in chapter 2.1.2. It was reported, that the two signals correlate in phase and the amplitudes are related by equation 2.14 on page 10. These estimations are routinely carried out and show a very good fit over a wide band of magnitudes and distances, as stated in e.g. Igel et al. (2007).

Ring laser design

Ring laser gyroscopes are active sagnac interferometers. The basic design is an enclosed cavity of triangular or (at the laboratories of our working group) rectangular shape, filled with a mixture of ^{20}Ne, ^{22}Ne and ^{4}He gas. The gas mixture represents the laser gain medium for the HeNe laser, which possess a high frequency stability and are the most powerful lasers for continuous operations. Stainless steel pipes are used to establish the capsuled tube system. At the gain tube (see figure 2.1 page 17, "laser excitation") the lasing process is initialized by a RF discharge. Two independent laser beams are generated, travelling in opposite directions on the same beam path, which is established by the supermirrors situated in each corner of the cavity. In order to obtain the rotation rate, at one of the corners the two laser beams are combined and superimposed using a laser beam pickup system, explained in section 2.3.6, page 18.

A prerequisite for the detection of the sagnac signal is for the instrument to operate in the monomode regime. The variations in cavity length due to expansion or contraction must not exceed one wavelength (633 nm), in order to achieve only one longitudinal

mode for each sense of direction.
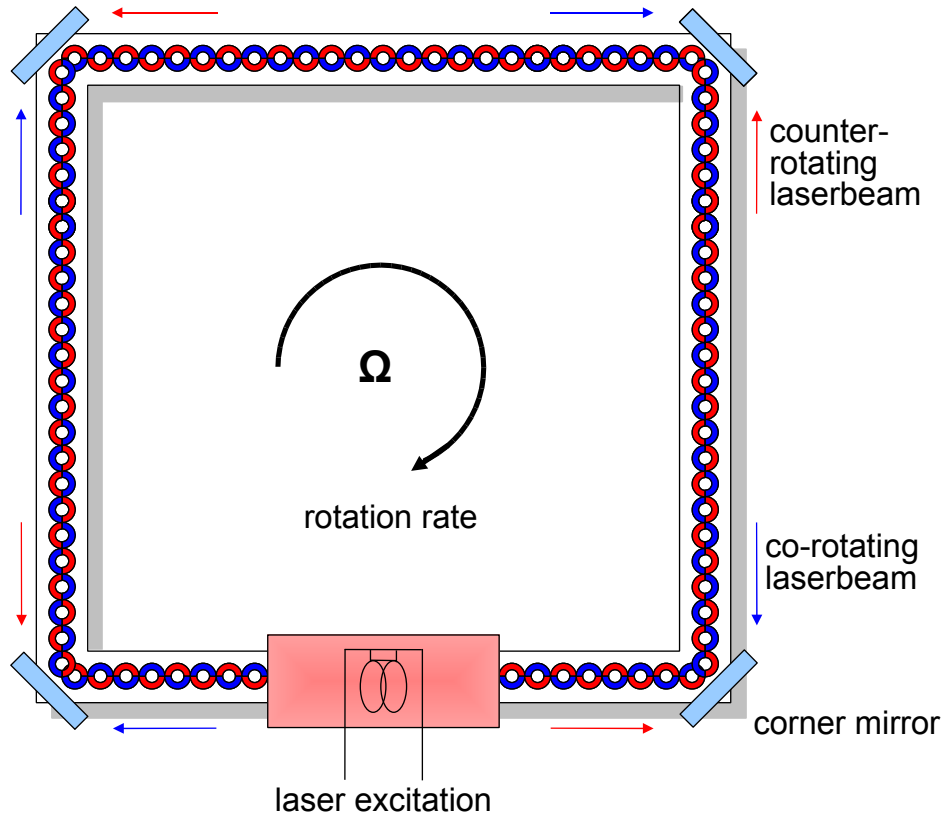
Figure 2.1.: This schematic shows the principle of ring laser operation. The corotating (blue) and counterrotating (red) light beams travel inside a closed tube system, with a superreflecting mirror positioned at each corner.

Previous studies reported ring lasers sensitivity to variations of ambient temperature, pressure and humidity. As the accuracy of the obtained signal depends on the mechanical rigidity (Schreiber et al, 2005) of the tube system, a suitable environment, such as an underground laboratory providing a stable level of environmental influences, is crucial. The ring lasers installation location must also provide a high quality surface (e.g. a concrete pillar, bedrock or Zerodur®) with a flatness of better than 1mm (Velikoseltsev and Schreiber, 2005), power supply and internet connection. Continuous operation of the gyroscope requires additional equipment, like control electronics e.g. for the beam power stabilisation, a detection unit for the sagnac frequency and a data acquisition unit including internet access.

Laser beam pickup system
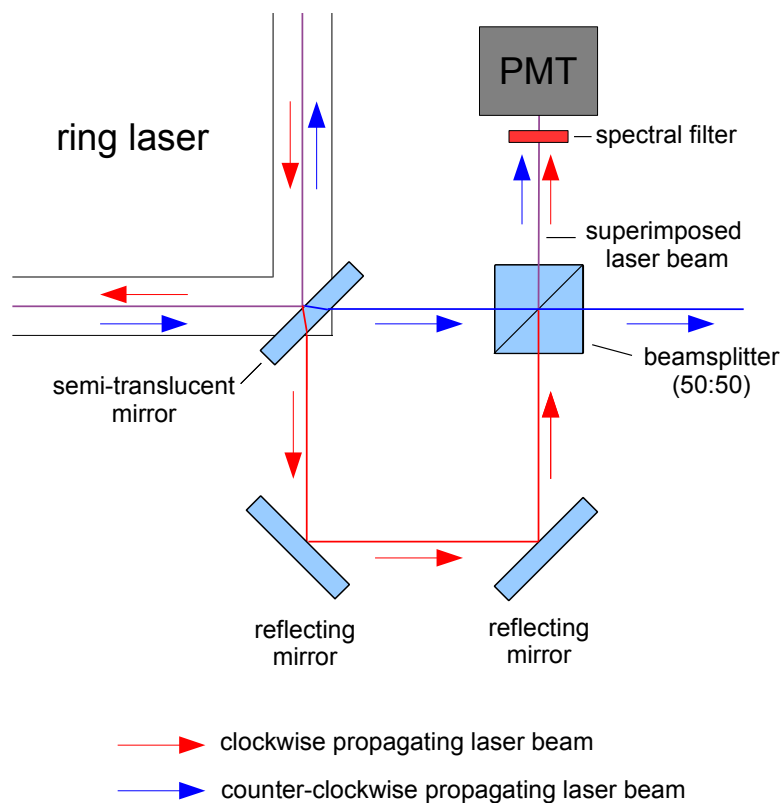
Figure 2.2.: The pickup system: the counterpropagating laser beams pass through a semitranslucent mirror at one the cornerboxes. The signals are superimposed in order to obtain the beat frequency, which is detected by a photodiode (PD) or a photomultiplier (PMT).

Located at one of the corners, a system superimposing the two counterpropagating laser beams is situated. The mirror inside this cornerbox is semitranslucent and allows a part (approx. 0.2 ppm) of each laser beam to pass through (see figure 2.2 on page 2.2). An array of mirrors is needed to overlay the two beams using a 50:50 beamsplitter. The superimposed signal is the beat frequency of the counterpropagating laser beams. After passing through a narrow band spectral filter (10nm), this frequency, which is proportional to it, is detected by the PMT or PD as a quickly changing series of light and dark (interference fringes) and converted to an electrical signal (voltage) proportional to the beat frequency. Measuring the fringes accurately is the main requirement for generating a precise electrical signal therefore a high contrast of the superimposed signal is desirable. Low contrast leads to insufficient frequency estimations, caused by low and noisy amplitudes. A close to perfect positioning of the mirror system and laser beams, which is generating a highly precise superposition, is desired.

Ring laser cavity quality

One of the most important parts in a ring laser gyroscope are the supermirrors and their reflectivity. The so-called 'ringdown'-experiment, where the laser light intensity is determined by a photo multiplier and converted to a ('signal'-) voltage, allows us to determine the mirror quality. Here the decay time τ, which is the period of time from the instantaneous shutdown of the laser to the approach of 1/e of the ('signal'-) voltage, is defined.

The quality factor Q of the cavity results as

$$Q = 2\pi f \tau, \tag{2.18}$$

with f being the optical laser frequency and τ the decay time.

Technical problems

Ring laser technology has undergone a massive development in the last decade. The high resolution received with these instruments was (and still is) a technical challenge. As mentioned in the section 'Ring laser design', a ring laser gyroscope must operate in the monomode regime. However, in gyroscopes, more than one longitudinal mode can be excited in each direction of propagation. Variations in cavity length are a critical factor, influenced by ambient temperature, pressure and humidity. A significant change in cavity length can lead to 'mode hopping' (longitudinal mode of both laser beams changes) or 'split mode' (longitudinal mode of one of the laser beams changes) operation and loss of the sagnac signal (figure 2.3). These effects are most often the reason for data loss. Very large ground motions (e.g. close to the source) can lead to similar effects, as a significant variation in cavity length may allow a new integral number of wavelengths to fit inside the cavity.

A number of operational problems have still to be overcome, such as the backscattering and the 'lock-in' effect (Stedman, 2001). The gas mixture inside the cavity undergoes an aging process, forcing to raise the beam power slightly over time, until the system has to be filled again. A similar process can be reported for the supermirrors, where the aging process decreases the reflectivity. As this technology is fairly new, solutions for the technical problems are expected to be provided over the next years, increasing the running stability and accuracy of the measurements.
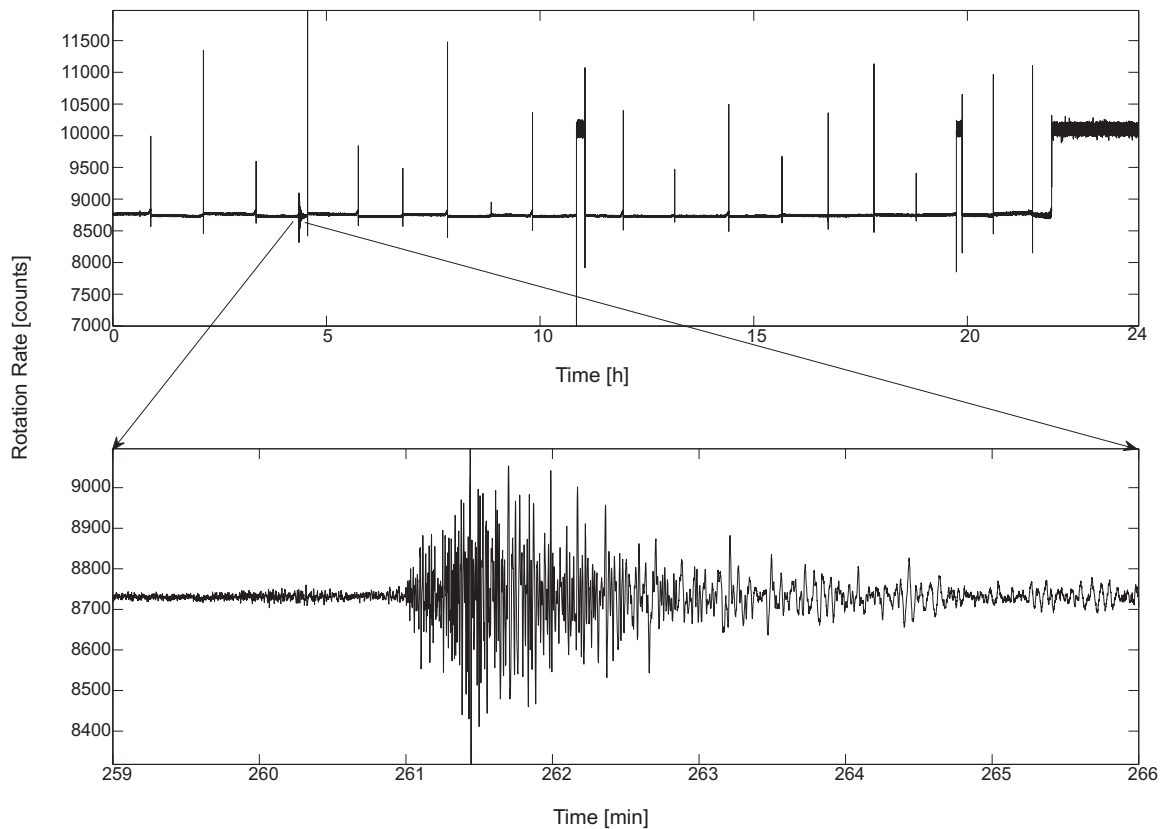
Figure 2.3.: The top figure shows the 24 hours data from the Piñon Flat observatory on 24th of May 2006. Here the 'mode jumps' ('mode hopping') and split mode operation is clearly visible. The bottom figure shows an event recorded in a section of regular ring laser operation.

2.4. Conclusion and future outlook

We state that instruments which detect rotational motions by employing the sagnac effect show a very high applicability for seismology and offer the possibility to record long term seismic data. In this thesis, the main focus is laid on ring laser gyroscopes, as their very good data quality has been proven in other studies. For those instruments a suitable environment will always be essential in order to realize long term running stability and data acquisition. A three component ring laser system would provide the means to measure all components of rotation at a very high level of resolution. With next generations of this technology to come, resolution, long term running stability and data quality will increase, while the costs for those instruments will decrease significantly. Mobile rotation sensor arrays providing less resolution are more likely to be implemented using fibre optic gyroscopes.

Chapter 3.

Instrumentation

This chapter focuses on the three ring laser observatories located in Christchurch (New Zealand), Wettzell (Germany) and Piñon Flat (US) and their instrumentation. Due to the recent development in ring laser technology, this technique became useful not only for geodesy but also for geophysics. Intentionally geodesists desired to determine variations in earth's rotation rate by applying ring laser technology. Based on the ever increasing sensitivity seismologists considered the measurement of rotational motions created by earthquake waves with these instruments. Over the last decade several studies showed that ring laser gyroscopes possess the power to detect rotational motions over a wide band of frequencies and magnitudes and the full consistency of collocated measurements of translations and rotations. At the laboratories mentioned here, there are altogether five (active) ring laser gyroscopes, listed in table 3. All of these devices are HeNe-laser with a wavelength of 633 nm.

Table 3.1.: Basic data on the ring laser gyroscopes located at the laboratories of our working group.

ring laser	perimeter	size	lat	lon	f_s
C-II	4 m	$1m^2$	$-43.57475°$	$172.62328°$	79 Hz
(UG-I	76.93 m	$366.86m^2$	$-43.57475°$	$172.62328°$	1512 Hz)
UG-II	121.09 m	$834.12m^2$	$-43.57475°$	$172.62328°$	2177 Hz
G-0	14 m	$12.25m^2$	$-43.57475°$	$172.62328°$	288 Hz
G	16 m	$16m^2$	$49.1450°$	$12.8780°$	348 Hz
GEOsensor	6.4 m	$2.56m^2$	$33.6090°$	$-116.4553°$	102 Hz

These devices vary significantly in size and location. The mentioned fit in phase and amplitude can be reported for the 'G' ring laser at the Wettzell observatory and is similarly expected for the other locations.

3.1. The Wettzell observatory

At the Fundamentalstation Wettzell, located in the north-west of Bavaria, basic research in various sciences is carried out. Amongst other laboratories, this facility is home to the most sophisticated ring laser observatory worldwide. The advanced system is, due to its high sensitivity, ideally suited for the detection of teleseismic events. Furthermore the location offers a very low noise level.

3.1.1. The underground laboratory

This large scale underground laboratory was specially designed and build for ring laser applications at the border of the Fundamentalstation Wettzell (see figure 3.1, the exact position marked by the yellow square). In order to guarantee an optimal running
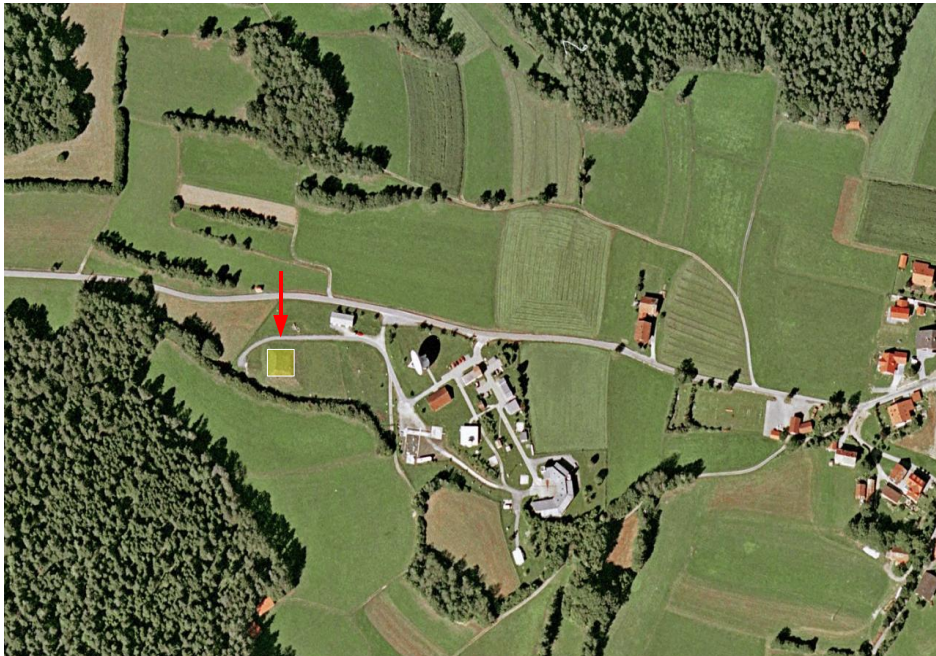
Figure 3.1.: Satellite view of the Fundamentalstation Wettzell, the underground location of the 'G' ring laser is marked by the yellow square.

stability for this high sensitivity instrumentation, the protection from variations of environmental influences was the major goal of this endeavour. In figure 3.2 the complex construction of the concrete monument is visible. The ring laser itself rests on a polished granite table with a thickness of 0.6 m which is situated on a massive concrete pillar attached to massive rock in a depth of approx. 10 meters. The temperature inside the cavity levelled of at 12.2 $°C$, with a seasonal variation of less than 0.6 $°C$. The electronic equipment - pressure control, data acquisition, power supply and network
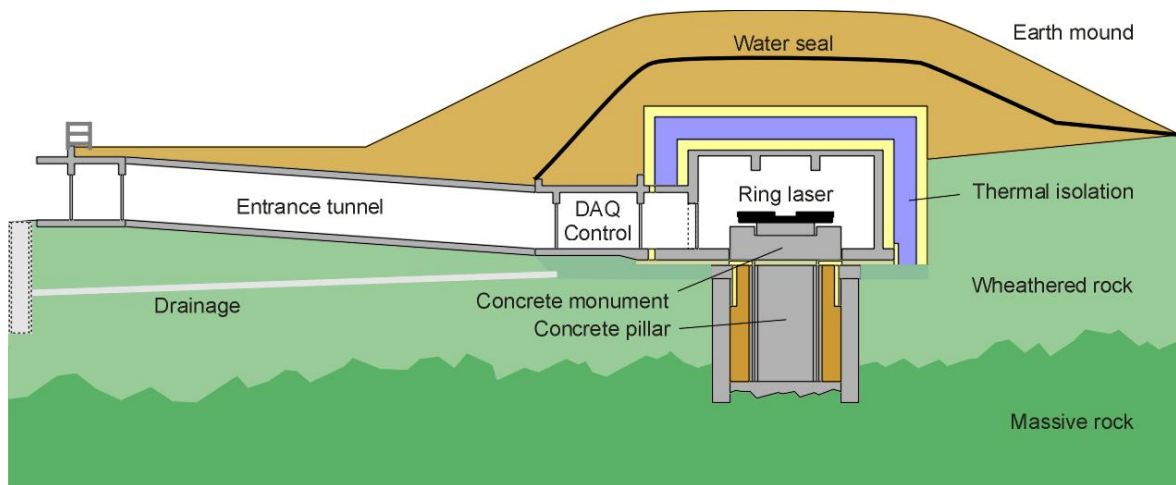
Figure 3.2.: Schematics of the underground laboratory at the Fundamentalstation Wettzell. The gyroscope itself is positioned in an environment assuring optimal conditions for stable long term measurements. (Wettzell, 2008)

connection - is located outside the main chamber to keep changes in ambient influences and the noise level as low as possible.

3.1.2. Instrumentation

Mounted at the underground observatory, the 'G' (Grossring) ring laser detects rotational motions around the vertical axis. In mid 2007, a collocated large scale fibre optic gyroscope has been installed there as well, detecting rotations around the same axis for comparison. The unique chance is offered to compare an active and a passive sagnac interferometer directly.

The ring laser gyroscope

The 'G' ring laser is momentarily the most sensitive and accurate instrument for the detection of rotational ground motions. This HeNe-laser was commissioned in 2001 with an effective area of 16 m^2 and a sagnac frequency of approx. $\delta f = 348.6 Hz$. The system is manufactured in a semi-monolithic design to guarantee high system stability. As visible on figure 3.3 on page 24, this device consists of four Zerodur$^®$ bars attached to a massive Zerodur$^®$ base plate, realizing a side length of 4 m. The Zerodur$^®$'s coefficient of thermal expansion is as low as $1 \times 10^{-8} K^{-1}$. In order to reduce backscattering effects, the slightly concave mirrors are of very high quality, allowing for losses of a few ppm only. Control electronics constantly monitor the beam power which is kept at a constant level employing a feedback loop. Due to the 'high
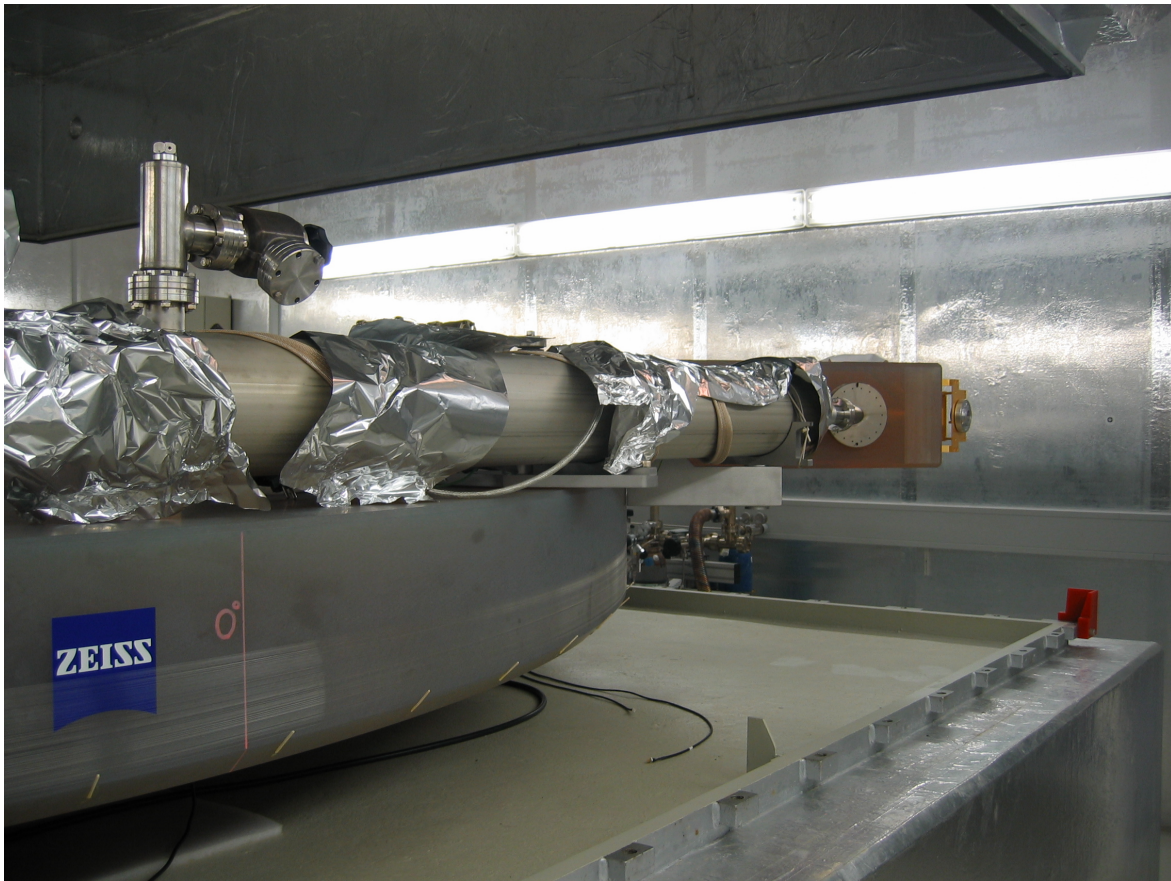
Figure 3.3.: This figure shows the 'G' ring laser at the Fundamentalstation Wettzell; a fibre optic wire with a length of approx. 2 km length is winded around the plate of Zerodur®.

end' solutions concerning construction and location this instrument is currently the most accurate ring laser gyroscope available with a sensitivity of $9.1 \times 10^{-11} \frac{rad}{s\sqrt{Hz}}$. Though, mathematically its sensitivity is exceeded by 'UG-II' with $7.3 \times 10^{-12} \frac{rad}{s\sqrt{Hz}}$, the effects of backscattering and ambient influences reduce the actual signal quality of the Canterbury ring laser. Since its startup, several large teleseismic events were recorded, see e.g. Igel et al. (2007). Also the first comparison between directly detected and array derived rotational motions was conducted with this system in 2003/2004 (Suryanto et al., 2006).

The fibre optic gyroscope

In order to capitalize from the extremely well designed location, a few km of fibre optic wire were winded around the Zerodur® base plate of the ring laser (lower part of the Zerodur® base plate in figure 3.3), creating a very large fibre optic gyroscope. Currently the quality of the recorded data is being investigated and compared to the

measurements of 'G'.

The seismometer

The instrument recording translational ground motions is a Streckeisen STS-2 broadband seismometer (with a corner frequency of 0.00833 Hz and a sensitivity of 1500 V/s/m), which is part of the GNRS, the *German Regional Seismic Network*. Its data can be found on the website: http://www.erdbeben-in-bayern.de/.

Additional equipment

Additional to the mentioned instruments, six Lippmann tiltmeters are positioned on the ring laser gyroscope, as changes in **n** (see equation 2.17 page 16) contribute to the rotation signal detected by 'G'. Ambient parameters like air pressure, temperature and humidity are constantly monitored as well.

3.1.3. Data acquisition

The acquisition system at the laboratory in Wettzell makes a broad band of data sets at different sampling rates available for scientists. The ring laser data is, similar to Christchurch, converted by a photodiode ('PD' in figure 3.4 on page 26) into an alternating voltage (which has a frequency similar to the sagnac frequency). A signal splitter allows for a simultaneous sagnac frequency estimation applying different methods:

(1) The voltage is digitized and frequency estimation is carried out by the so-called **AR(2)-analysis** (*auto regressive second order analysis*. This method needs a minimum length of the obtained dataset and works for teleseismic events with slowly changing frequencies only (see Velikoseltsev and Schreiber (2005)). As the raw data has to be bandpass filtered, this approach is not suitable for higher frequencies. The data is stored with a sampling rate of 3s and 30s respectively, which is useful for geodesists to detect changes in earth's rotation rate.

(2) An analogue frequency determination is realized by a **FMD** - a Frequency Demodulator which is basically the same as a PLL - a Phase Locked Loop. The incoming signal is sampled at 1 kHz. A PLL generates a signal (voltage), that corresponds in phase and frequency to the incoming signal of the ring laser - without time delay. As long as no additional signal than the earth's rotation rate is obtained, the voltage controlled oscillator is phaselocked to the beat frequency, using a constant control
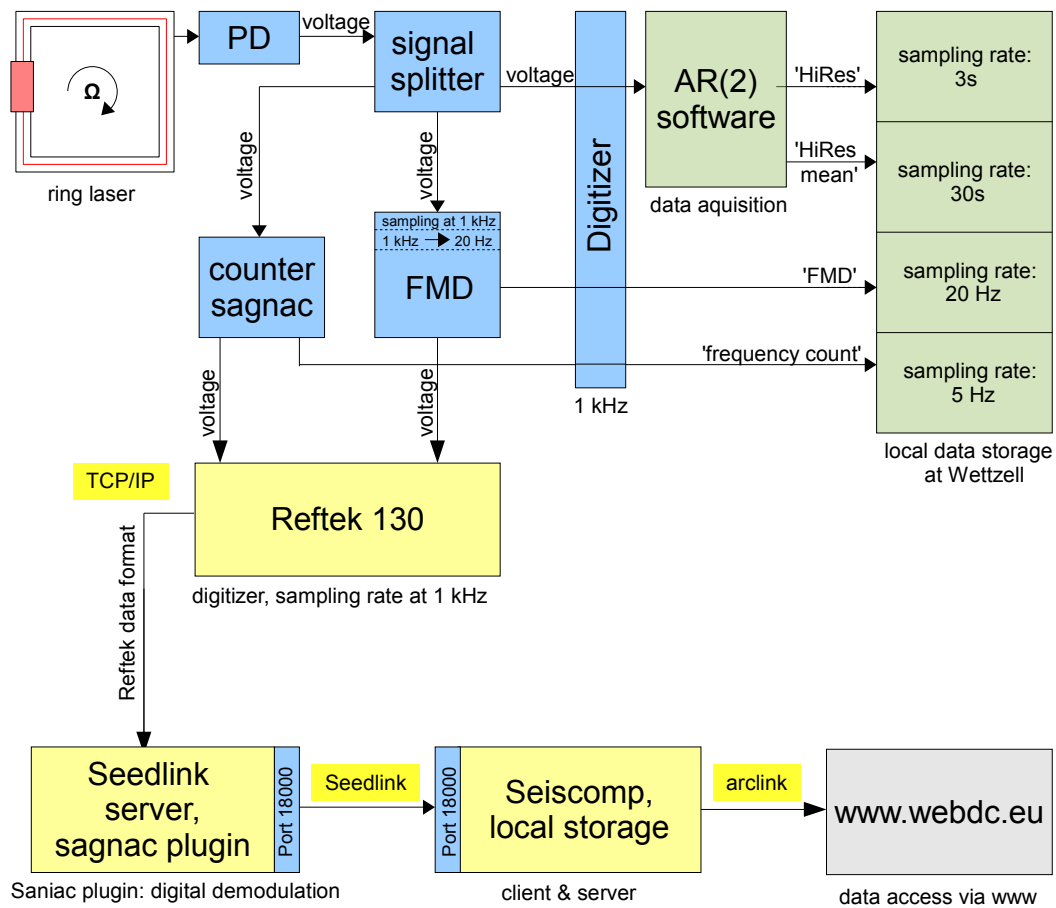
Figure 3.4.: Schematics of the data transfer and acquisition system at the Wettzell laboratory.

voltage. Once an additional (seismic) signal is detected by the gyroscope, the change of the sagnac frequency leads to a misfit between reference signal and sagnac signal. A feedback loop adjusts the oscillator signal, keeping the phase locked. The feedback loop signal is therefore directly proportional to the incoming signal, which represents the change in rotation rate. As the signal needs to be consistent with other seismic recordings, the voltage is sampled at 20 Hz and stored locally at Wettzell.

(3) The third way of frequency estimation is the use of a **sagnac counter**. The frequency is estimated simply by the counting the incoming number of waves and dividing it by a specific time, which is called 'gate time'. The gained data is digitized and stored with a sampling rate of 5 Hz.

(4) Since end of March 2007, a near real time data connection was established using the **SeedLink and ArcLink** software. The raw data is sampled (1 kHz) and digitized by a 'Reftek 130' and then digitally demodulated by the use of the 'sagnac plug-in'.

Table 3.2.: Sagnac frequency estimation systems for the corresponding frequency bands.

frequency estimation method	resolution
frequency counter	up to 1 Hz
AR(2)	up to 4 Hz
FMD	full seismic band

This acquisition technique offers a much better signal/noise-ratio than the analogue demodulation employed by the 'FMD'. The accuracy of the phase determination, using the analogue demodulation, depends significantly on the length of the phase estimation time window. For slowly changing frequencies, a long time window can be applied which enlarges the bandwidth but results in an unexact estimation, as fast changes cannot be registered. For higher frequencies a shorter time window is applied which limits the bandwidth and increases the noise level.

The digital demodulation determines the instantaneous frequency at the time t in the seismogram, which delivers a much lower noise level and higher accuracy of the estimation. The determination of the instantaneous frequency is carried out by the approximation

$$f_i = \frac{x_i(t)\frac{d}{dt}x_{H_i}(t) - x_{H_i}(t)\frac{d}{dt}x_i(t)}{2\pi x_i x_{H_i}}, \tag{3.1}$$

where

$$x_i(t) = A(t)cos\Theta(t) \tag{3.2}$$

is the seismogram (A(t) is the amplitude and $\Theta(t)$ is the phase) and

$$x_{H_i} = A(t)sin\Theta(t) \tag{3.3}$$

is the imaginary part of $x_i(t)$ (H standing for Hilbert transform). This and the 'FMD' dataset are stored on a server at the seismological observatory in Fürstenfeldbruck (Germany) with a sampling rate of 20 Hz. The data can be accessed online (via *ArcLink*) on the 'webdc' website: http://www.webdc.eu. In table 3.2 the fields of application for the different frequency estimation systems are displayed.

3.2. The Christchurch observatory

Positioned on the east coast of the south island of New Zealand, the city of Christchurch is situated close to the tectonically very active plate boundary of the Australian and the Pacific Plate. In an underground laboratory the worldwide largest ring laser test facility, which is operated by the University of Canterbury and the Fundamentalstation Wettzell, is situated.

3.2.1. The underground laboratory

Located at the southern outskirts of Christchurch, the 'Cashmere Cavern' was build during World War II by the New Zealand military and has a size of about 50m × 30m. This test facility serves as home to the ring laser project since the late 1980s and the first ring laser experiments were carried out here. Today the caverns have been converted to an underground observatory housing the ring lasers, a standard three axis seismometer and the required electronical equipment. This laboratory offers power supply, since the recent past internet connection and the seismic and thermal stability required for such a test facility. Here the worlds largest ring laser (named UG-II) with an area of 834.12 m^2, as well as the only ring laser measuring rotations around a horizontal axis (named G-0) is located. As the site was of no special interest after World War II, the rock walls are still only partially covered by concrete, as the bunker was never fully finished back then. In figure 3.5 the location of the underground

Figure 3.5.: Christchurch satellite image (google earth) of the southern outskirts of Christchurch, New Zealand.

cavern is shown, the yellow square marking the approximate position 30 m below the surface. The exact position is 43.57475° South and 172.62328° East. The next sections are dedicated to the instruments employed at the Christchurch laboratory. Three ring laser gyroscopes measure the rate of rotation around a vertical axis of rotation, one instrument is sensitive to rotations around a horizontal axis. Therefore the unique opportunity of collocated measurements around two axes of rotation is given, in an environment with stable ambient influences and a very low noise level.

3.2.2. Instrumentation

The next subsections give detailed information on the ring laser gyroscopes and the additional equipment stationed at the Cashmere Cavern. The naming convention for the gyroscopes is based on 'C' for 'Canterbury' and 'G' for 'Grossring'.
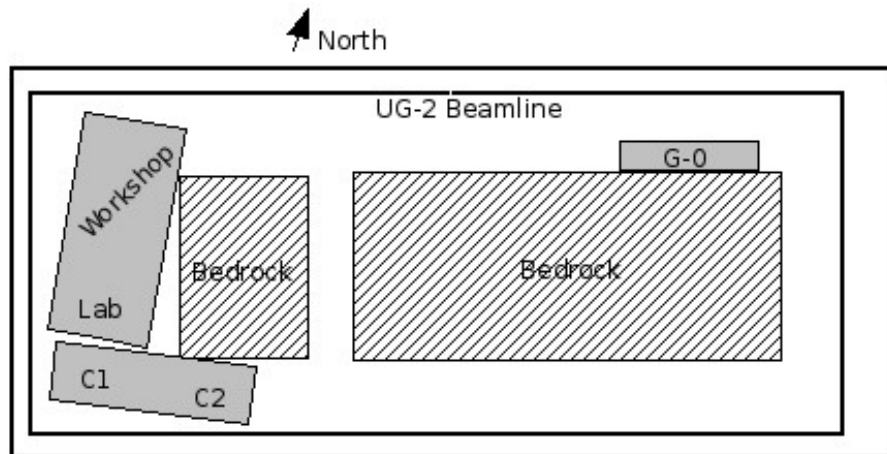
Figure 3.6.: Schematics of the Cashmere Cavern in Christchurch, New Zealand (Cashmere, 2008).

The ring laser gyroscope prototype 'C-I'

This HeNe laser was developed between 1987 and 1997 by the University of Canterbury and the Oklahoma State University. The prototypes' construction led to the conclusion, that large ring laser gyroscopes, with a perimeter of more than 0.6 meters can be used as sagnac interferometers. The instrument has an effective area of 0.7547 m^2 and the system is mounted on a plate of Zerodur®, minimising thermal drifts and mechanical vibrations (UC (2008) ring laser website). With a size of the plate of 1.2 m× 1.2 m ×

0.025 m it is situated on a 700 kg block of granite. The system has a quality factor (see equation 2.18) of

$$Q = 7.5 \times 10^{10} \tag{3.4}$$

but was never used for geoscientific applications due to its mechanical instability. Its design, electronic equipment and the vacuum pump can be seen on figure 3.7.
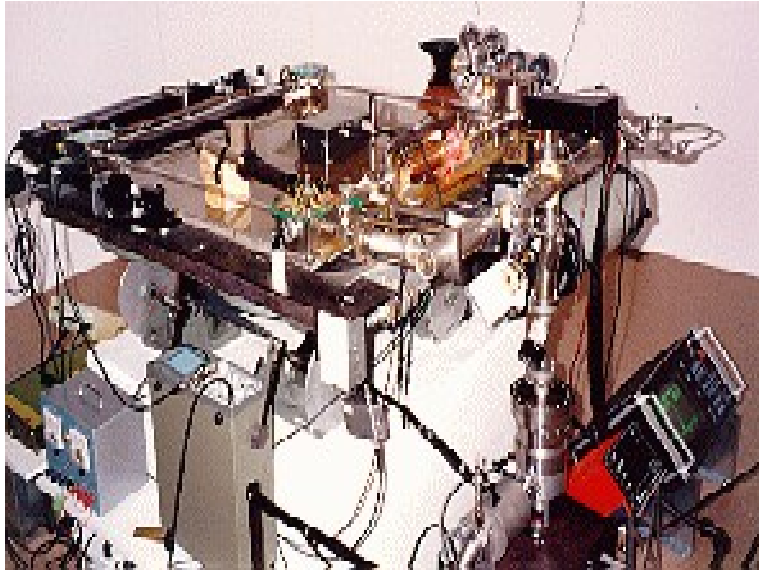
Figure 3.7.: Ring laser prototype 'C-I' at the Cashmere Cavern in Christchurch, New Zealand (C-I, 2008).

The ring laser gyroscope 'C-II'

The next generation gyroscope, with an effective area of 1 m^2 was constructed in collaboration with Carl Zeiss Inc. in 1995 and 1996 based on the knowledge gained from the 'C-I' ring laser. 'C-II' was developed as a prototype rotation sensor for geoscientific applications with sophisticated electronic control systems for frequency (and amplitude) stabilization and sagnac signal detection, maximizing signal quality and running stability.

Several scientific questions, like the feasibility of a monolithic design and the techniques for the implementation of a large ring laser were answered by this project. The ring laser cavity is drilled into a monolithic block of Zerodur® (located inside a pressure case), which has a size of 1.2 m× 1.2 m × 0.18 m. After its evacuation (ultra high vacuum) the cavity is filled with He and Ne gas as gainmedium. The system itself rests on a granite plate (thickness 0.2 m) which is situated on a massive concrete block with

a sidelength of 1.5 m. The quality factor increased to

$$Q = 5 \times 10^{11} \tag{3.5}$$

and earths rotation rate at the point of deployment is given as a sagnac frequency of $\delta f = 79.4 Hz$. Though this active sagnac interferometer was designed only as a
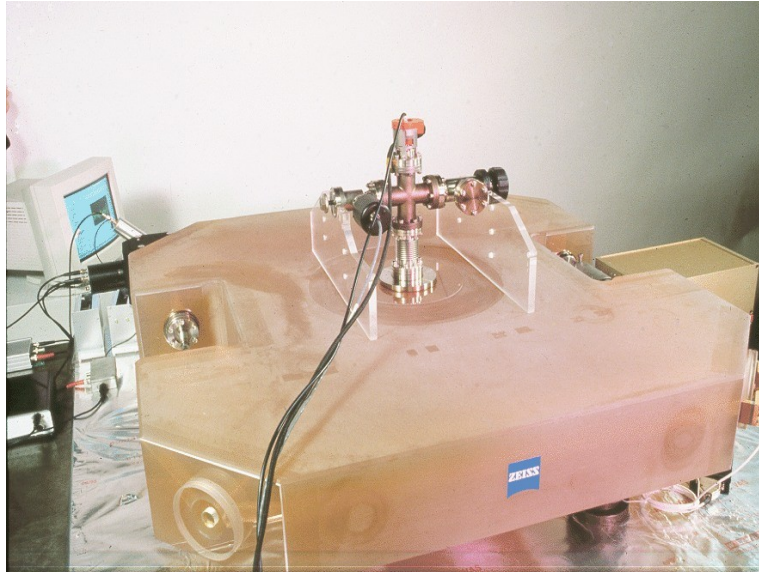
Figure 3.8.: Monolithic Zerodur$^{\circledR}$ cavity of the Canterbury ring laser 'C-II' (C-II, 2008).

prototype for an even larger ring laser gyroscope (the 'G' ring laser in Wettzell (Germany)), the recorded data verifies its applicability for geophysical research and is visualized on the webpage of the 'International Working Group on Rotational Seismology': http://www.rotational-seismology.org/data.

The ring laser gyroscope prototype 'G-0'

In 2000, after the operability of large ring laser gyroscopes had been tested by the 'C-II' project, it was still an open question, whether a ring laser with a planned size of 16 m^2 ('G', Wettzell) could be operated in the monomode regime. The prototype system 'G-0' was therefore developed to test mechanical stability and characteristics of a large perimeter ring laser. This gyroscope is square shaped, has an effective area of 12.25 m^2 and is vertically attached to one of inner walls (in E-W direction) of the observatory. The system consists of stainless steel pipes mounted to the cornerboxes housing the mirrors (see figure 3.9 on page 32). The material Zerodur$^{\circledR}$ was not applied. Intentionally this gyroscope was not designed for the use in geoscientific applications

Figure 3.9.: Large perimeter ring laser vertically attached at the Cashmere Cavern, Christchurch, New Zealand (G-0, 2008).

due to the design and mechanical instability. The quality factor of this instrument is in the range of $Q = 10^{12}$ and earths rotation rate can be seen at a sagnac frequency of $\delta f = 287.3 Hz$. Due to its high running stability, good data quality and the fact, that 'G-0' is the only large perimeter ring laser detecting rotational ground motions around a horizontal axis, the system is still operated today and the data can also be found on the web at: http://www.rotational-seismology.org/data.

The ring laser gyroscope 'UG-I'

The large perimeter ring laser 'UG-I' was operable between the years 2001 and 2004. It had a size of 17.5 m$\times$ 21 m and was the largest active sagnac interferometer worldwide at that time. The cavity was, similar to 'G-0', realized by stainless steel tubes attached to the cornerboxes housing the mirrors. According to the sagnac formula (formula 2.17, page 16), the gyroscopes sensitivity rises with a growing effective area.

Figure 3.10.: Picture of the UG-I/UG-II ring laser, located at the Cashmere Cavern, Christchurch, New Zealand (UG-II, 2008).

However, instruments of this size inevitable face a number of essential problems. The alignment, which is absolutely crucial for a high quality optical signal, changes due to environmental parameters like temperature and pressure. As the system was too large for a monolithic architecture (or even a plate of Zerodur®), the pipes and cornerboxes were simply attached to concrete pillars. Therefore variations in the flatness of the basement play an important role, as well as a higher noise level. This instrument obtained the sagnac frequency at $\delta f = 1512 Hz$, which is a problem for standard logging systems with a sampling frequency of up to 1000 Hz. The scientific benefit of this instrument was a higher quality factor of

$$Q = 3 \times 10^{12}, \tag{3.6}$$

the collocated measurement of rotational motions around the vertical axis of two ring laser gyroscopes and the technical expertise.

The ring laser gyroscope 'UG-II'

In 2004/2005 the ring laser 'UG-I' was partially disassembled and then enlarged to its present size of $834.12m^2$. The cavity structure is equal to the one of 'UG-I' and the modular design of steel pipes facilitated the extension. Following mathematical notations, this system has the highest resolution and sensitivity for the detection of seismically induced ground rotations. However the gyroscope has to cope with the same problems as the first generation. The sagnac frequency of 'UG-II' is very high at $\delta f = 2177Hz$. The sampling of this frequency is conducted by an adapted LabView coded data acquisition programme at the observatory. However, momentarily this frequency does not allow for an online data transfer and visualization of the instrument 'UG-II'.

The seismometer

Collocated to the ring laser gyroscopes is a broadband three axis seismometer type Güralp CMG-3 ESP with a natural period of 30s and a sensitivity of 2000 V/m/s. The instrument is part of the New Zealand seismic network (GNS), and its data can be found on the GNS-website. At the same time three components of translation are streamed on the harddrive of the acquisition computer at the laboratory at a sampling rate of 1000 Hz.

3.2.3. Data acquisition

The data logging and acquisition system in Christchurch can be divided into two branches (see figure 3.11 on page 35):

The LabView logging system was designed exclusively for the recording the sensor data in the Cashmere Cavern. The Sagnac signal detected by each ring laser is converted into an analogue voltage by a photo diode, digitized (at 1 kHz) and then streamed into a LabView coded logging programme. Synchronously the digitized (1 kHz) three components of the seismometer are recorded by the same programme. The resulting files show three components of translation and rotation, sampled at a frequency of 20 Hz. The logging system is compatible to the sagnac frequencies of all three ring lasers. Additional information on timing and external sensors is stored in these files as well. However, the data is stored locally on a harddrive and can not be accessed from outside (e.g. by a sftp connection).
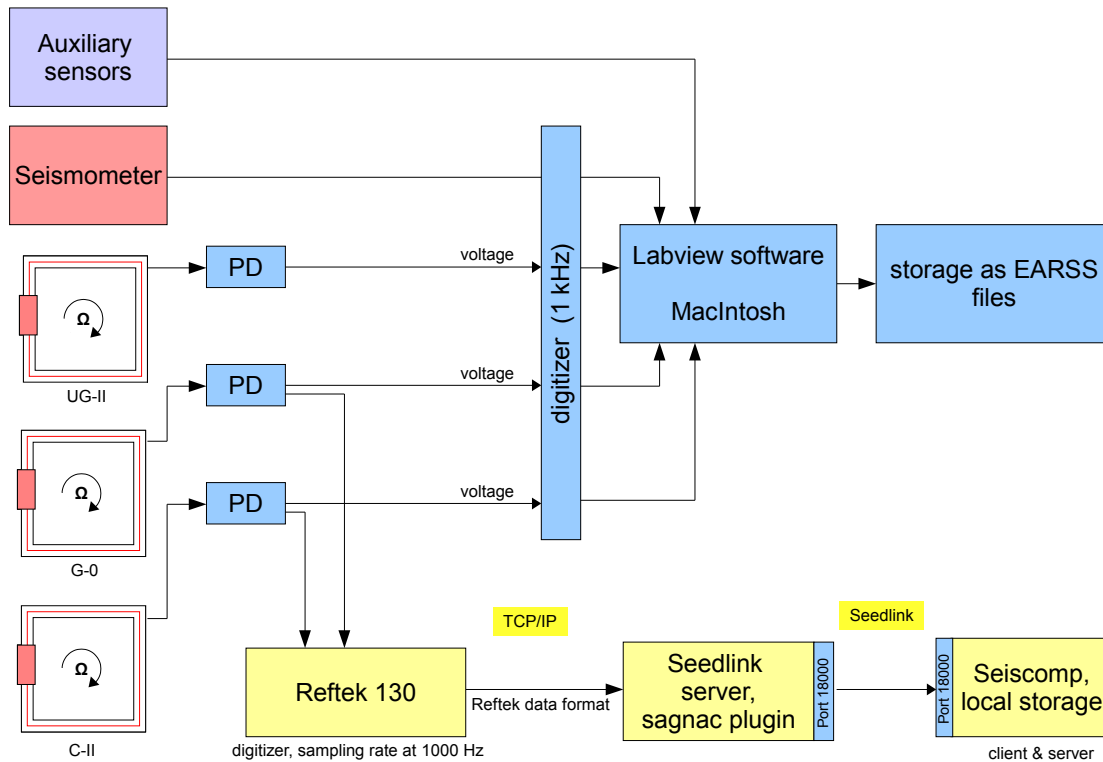
Figure 3.11.: Schematics of the data acquisition and transfer at the Christchurch ring laser laboratory.

Since late February of 2008 a **Reftek data logging system** is installed. The ring laser data of the systems 'C-II' and 'G-0' is send to a 'Reftek 130' broadband seismic recorder and digitized at 1 kHz. The recorders maximum sampling rate does not allow for a correct detection of the 'UG-II' sagnac frequency. The incoming data is converted into the 'Reftek' data format. Seedlink, a system (software) for real-time exchange between stations and data centres (GFZ, 2008), is employed to import the data from the 'Reftek 130' via the TCP/IP protocol. The 'sagnac' plug-in designed and developed in 2007 by Dr. J. Wassermann from the LMU München, (digitally) estimates the sagnac frequency. The benefit of this SeedLink system is the unified dataformat (miniSeed) which is transferred using the SeedLink transfer protocol to a server at the LMU München, where the data is stored as 24h files on the SeisComP server. As a precise timestamping is essential for the recorded data, a GPS receiver was installed at the Cashmere Cavern at the end of 2007.

3.3. The Piñon Flat observatory

Located remotely in the desert with a short distance to two of the most active faults in southern California, the San Andreas Fault (25 km) and the San Jacinto Fault (12 km), the Piñon Flat Observatory (PFO) is operated since the 1970s by the scientists of the University of California, San Diego (UCSD). Here the great possibility is offered to study earthquake processes from a very close proximity in an area that is known to be tectonically very active. The collocation of a various number of instruments allows the study of different components (e.g. translations, strain, tilt, rotation) at the same time. The installed instruments include: laser strain meters, borehole dilatometers, borehole strain meters, long fluid tiltmeters, optical fibre infrasound sensors, an optical fiber strain meter, borehole tiltmeters, an IMS infrasound array, an ANZA seismic network station, a realtime continuous GPS stations and recording system and the GEOsensor (ring laser gyroscope). Furthermore the facility serves as testing ground for newly developed geophysical equipment which is operated by investigators from all over the world.
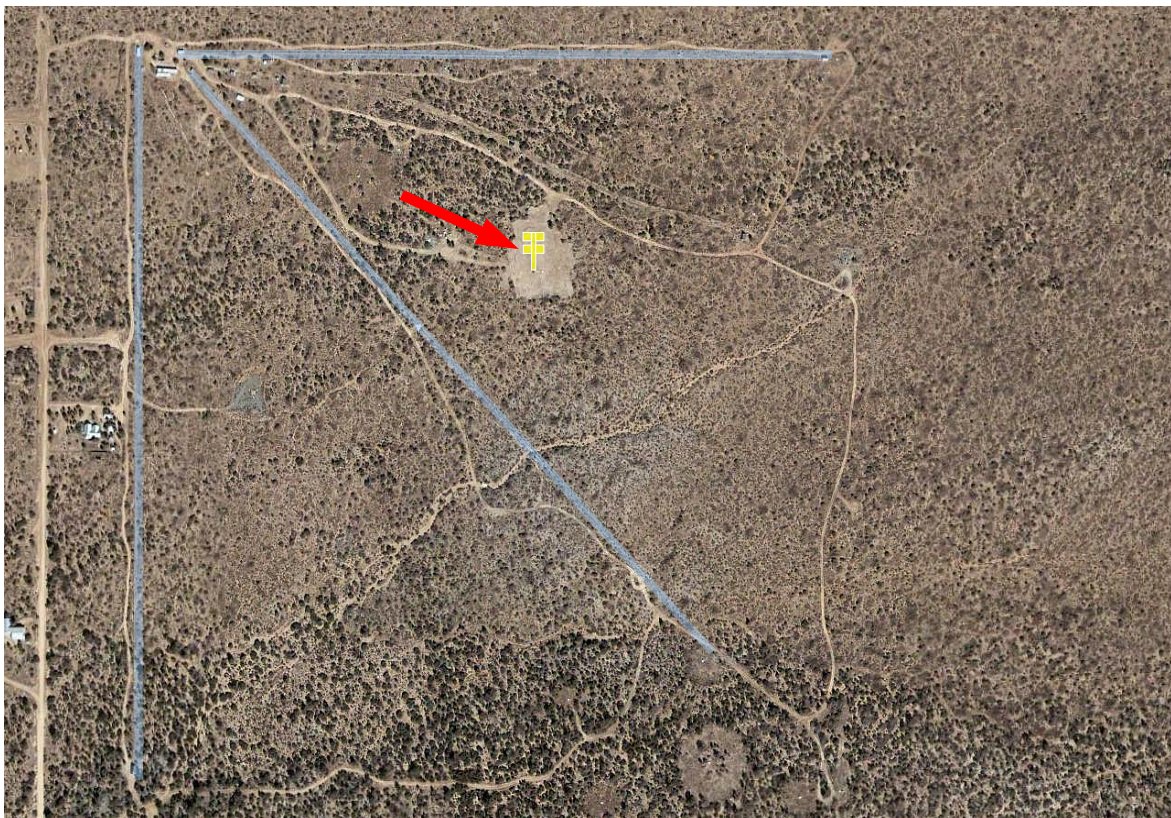
Figure 3.12.: On this satellite image (google earth) the strain meters with a side length of about 730 meters are marked blue, the seismic research facility marked yellow and the GEOsensor vault is marked by the red arrow.

In 2004 an underground seismic research facility was build at the testing ground, consisting of four chambers serving for instrument development purposes (see figure 3.12). One of the observing vaults now houses the ring laser gyroscope and the collocated instrumentation, which was used in this study.

3.3.1. The underground laboratory

The aim of building an underground research facility was to create an environment that provides essentials for seismic studies: low background noise, temperature stability, GPS timing, internet connection and power supply.

The four vaults are buried five meters deep, accessible via a 20 meter long ramp. The two chambers in the back were equipped with granite piers, the two in the front (in one of which the GEOsensor is located) were equipped with isolated concrete piers (see fig. 3.13). On the satellite image (google earth) of the PFO area (see figure 3.12) the laser strain meters with a length of more than 730 meters have been marked blue to visualized the size of the test facility. The location of the underground seismic research facility is illustrated by yellow rectangulars, with the red arrow pointing at the place where the GEOsensor is located.
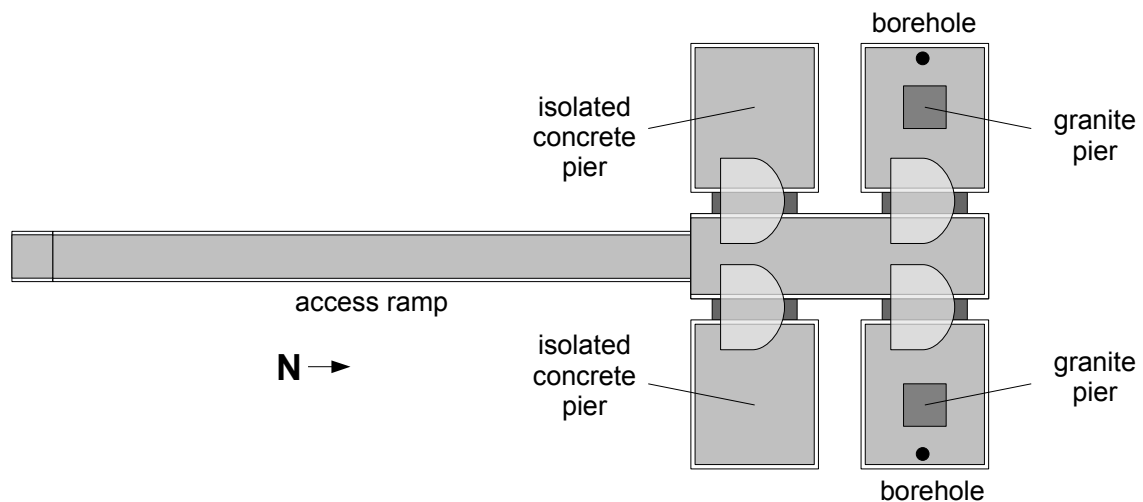
Figure 3.13.: Scheme (from top) of the Piñon Flat observatory, showing the access ramp on the left and the four seismic vaults on the right hand side. The GEOsensor is stationed in the top left chamber.

3.3.2. Instrumentation

The ring laser component of the GEOsensor measures rotational ground motions around the vertical axis. The system, which was designed for seismic and geophysical studies not only consists of a ring laser gyroscope, but also of a collocated standard three axis seismometer, two tiltmeters (N-S and E-W) and a GPS time reference (see figure 3.14).
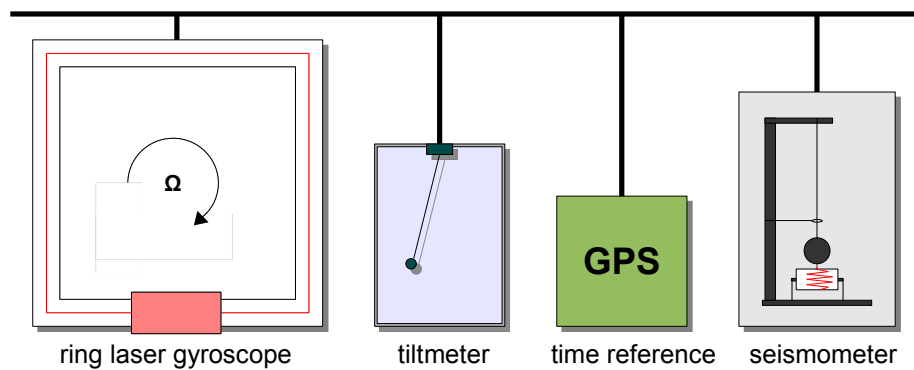
Figure 3.14.: Basic principle of the GEOsensor: a ring laser component, a tiltsmeter, a GPS time reference and a standard three axis seismometer.

The ring laser component

The ring laser component of the GEOsensor (see figure 3.14) is the first instrument of its kind that was specially designed for geophysical applications. It was constructed as trade-off between sensitivity, high stability and the benefits of a monolithic large ring laser design and mobility, montage flexibility and costs (Velikoseltsev and Schreiber, 2005). The systems has an effective area of $2.56m^2$ and a sagnac frequency at the site of deployment of approx. $\delta f = 102Hz$. Like the large perimeter ring lasers in Christchurch, the square shaped cavity is realized by the use of stainless steel pipes. Due to its modular design the ring laser can be enhanced simply by using longer steel tubes, which eventually meets sensitivity requirements in the future. The cornerboxes (figure 3.15, black with green plates) are attached rigidly to the concrete floor. The running stability of the gyroscope is ensured by a 'beampower stabilization' control loop. A PD is employed to deliver a voltage corresponding to the intensity of the laser beams. This voltage is connected to an operational amplifier and compared with a reference voltage. A feedback line voltage which controls the gain is increased and leads to a higher voltage at the RF discharge, as soon as the voltage coming from the PD drops.

Figure 3.15.: This picture shows the operable ring laser component of the GEOsensor with the gaintube in front (middle), the four cornerboxes (with the mirror holders inside) and the tiltmeter (in the back).

Improvement of the ring laser component

In November/December 2006 the feedback loop was upgraded, as the intensity of the light beams was too low for the PD to create a suitable signal for the control loop. Due to a PMT's much higher amplification factor (compared to the PD), the two devices were exchanged. Although the obtained sagnac signal has a lower intensity now, it is still strong enough for the sagnac frequency estimation. A correction to the control loop was installed also, which allows the adjustment of the gain remotely via the internet. This is a major step forward, as adjusting the gain level has to be carried out quite often.

The seismometer

Three components of ground velocity are measured by the collocated Lennartz LE-3D 20s seismometer, which returns the change in ground velocity as a varying DC voltage.

It has a corner frequency of 0.05 Hz and a sensitivity of 1000 V/m/s.

The tiltmeter

The tiltmeter is a LGM Lippmann with an angular resolution of 1 nrad. It measures two components (N-S and E-W) of change in orientation of the surface plane. Though the contribution of tilt is respectively quite small, usually not larger than a 5% contribution of the rotation rates, the signal still has to be accounted for.

GPS

A GPS receiver gives the time reference as frequency output and is an integral part of the system, as its signals are used for all the components. The data samples time stamping is provided with an accuracy of '30 ns relative to UTC' (Velikoseltsev and Schreiber (2005)), the accuracy of the reference frequency provided by the GPS receiver is better than $1 \cdot 10^{-12}$. The requirement of times tamping the data samples with an accuracy of at least 1 ms is therefore provided.
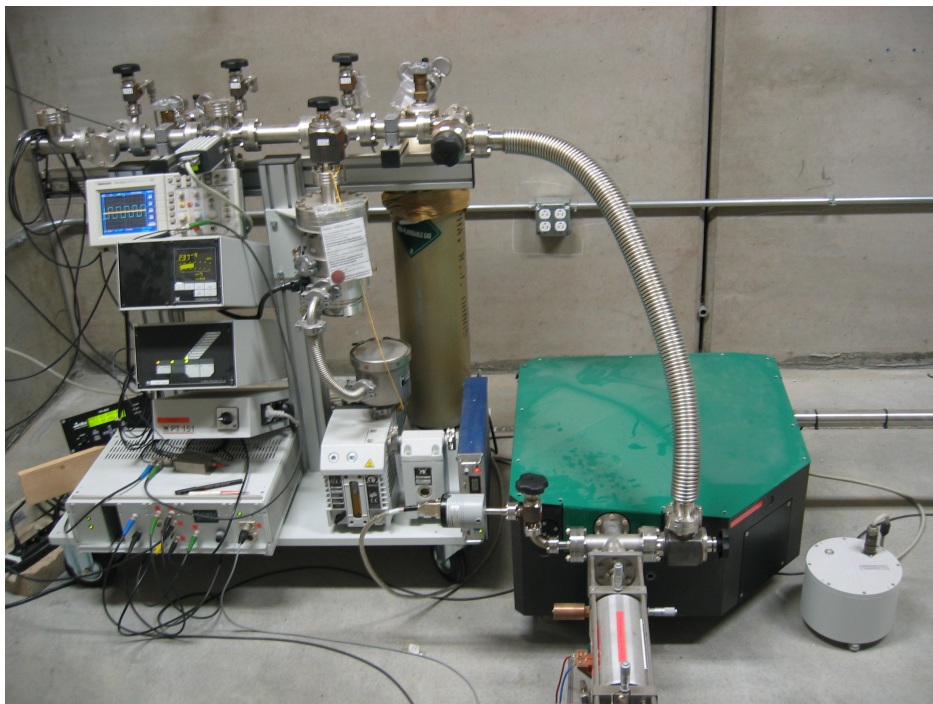
Figure 3.16.: This picture shows the electronic equipment, turbomolecular pump and the gas mixture system.

3.3.3. Data acquisition

At the Piñon Flat observatory the digitization and data acquisition is carried out by a computer, based on the PXI (Personal eXtension for Instrumentation) system. The machine possesses a 20 GB internal harddisk for temporary storage of the datasets created by the LabView coded logging programme. The major advantage of this system is reliability, as the controller serves for acquisition and communication only. The system can be accessed via the internet using a build-in ftp. Similar to Christchurch
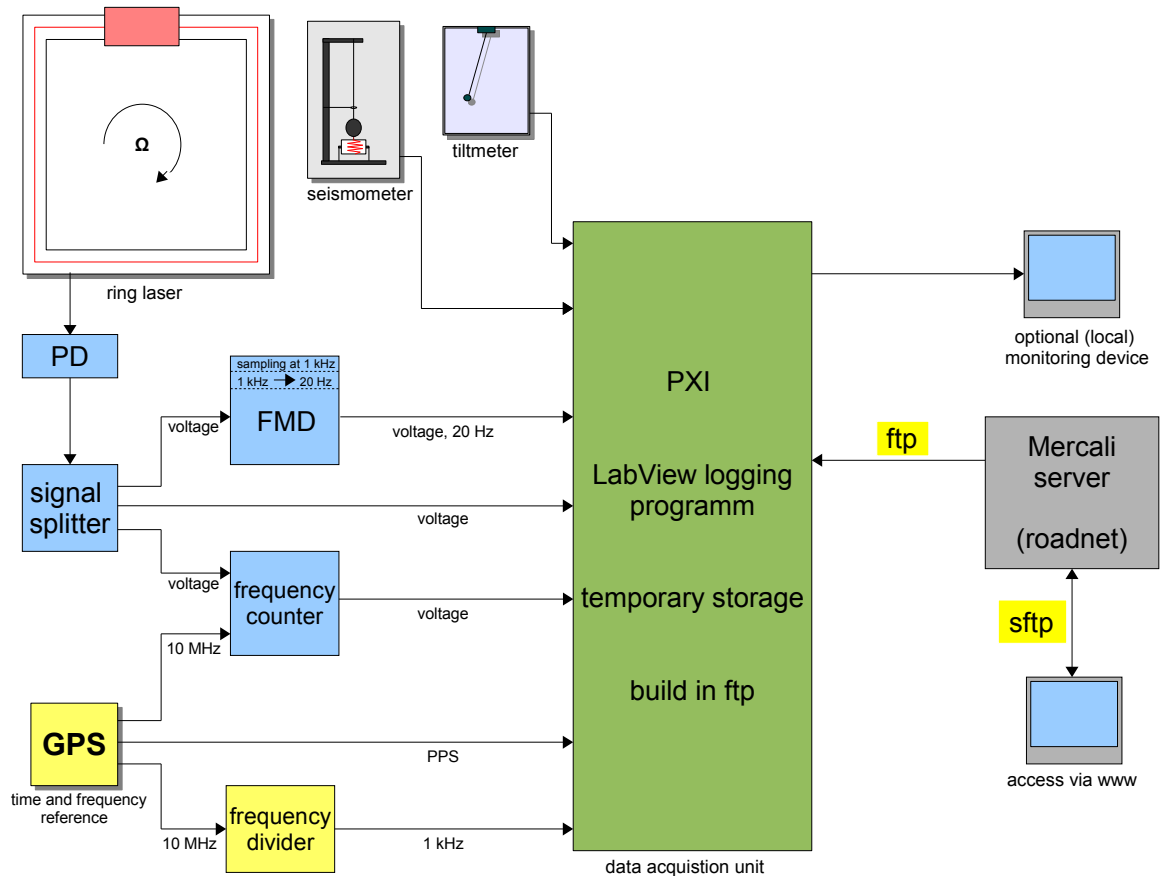
Figure 3.17.: Schematics of the data acquisition, storage and transfer system at the GEOsensor laboratory at Piñon Flat.

and Wettzell, the ring lasers output signal (beat frequency) is converted to a voltage with a frequency that corresponds to the sagnac frequency. This signal is split up into three channels by the signal divider, all channels carrying the same signal. In order to obtain the frequency variations, different frequency estimations are applied. As the sagnac frequency detection systems are similar to the ones at the Wettzell observatory, the techniques are not explained in detail.

The frequency estimations are carried out applying the **FMD**, **AR(2)** and **frequency**

counter applications, similar to the station in Wettzell. A GPS receiver functions as time and frequency reference. A 10 MHz signal is delivered to the frequency counter as reference signal and to a frequency divider. This device converts the 10 MHz down to 1 kHz, which is connected to the acquisition unit and serves as acquisition rate. The receiver also delivers a 1 PPS (pulse per second) signal to the acquisition computer, utilized for the time stamping. Additional data of the collocated seismometer and the two axis tiltmeter is digitized, sampled and stored by the PXI computer as well. However, during the acquisition process, which is 24h, the data is not accessible. The recorded data files are stored locally on the PXI machine, only accessible over ftp via the so-called 'mercali server' which is a part of the California 'RoadNet' system. The server is accessed using a sftp connection from any local computer. Although a 'Quanterra q330' datalogger is installed at the facility, which would allow for a near real time data transfer and display, however, this system could not be accessed.

3.4. Conclusions

The ring lasers referred to in this study vary in size and therefore in resolution. The most sensitive is 'G' in Wettzell, while the 'GEOsensor' is the one with the highest applicability to seismic observatory measurements. Whether a broadband rotation sensor can be used for nearfield and farfield observations remains to be determined by future studies. The application of ring laser technology in portable instruments used in aftershock and close to source regions is unlikely due to their high demand for a stable environment.

Chapter 4.

Towards a global network of rotation sensors
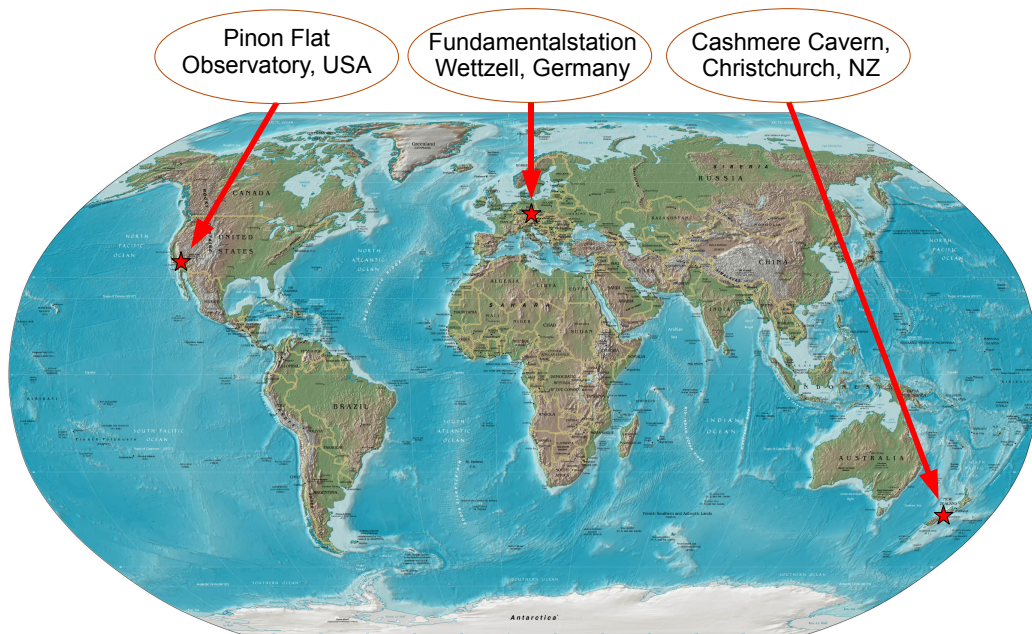
Figure 4.1.: Location of the three ring laser laboratories referred to in this thesis.

The previous chapter characterized the ring laser laboratories with a special emphasis on data acquisition, storage and transfer systems. In order to be useful for a broad range of investigations, the recorded rotation data need to be easily available for scientists worldwide. As rotational seismology is a new field of interest for geophysicists, geodesists and civil engineers, a near real time visualization of the recorded rotation data, similar to e.g. seismometer recordings, attracts attention and arouses interest. On top of that, an estimation of the data quality can be carried out simply by comparing rotational with translational seismograms online. Therefore a major goal of this thesis was to realize a permanent data flow from each of the stations. A unified data

portal is eligible (e.g. http://www.webdc.eu), allowing the access to long term data in a standardised data format. Figure 4.1 on page 43 presents the distribution of ring laser laboratories where an online data visualization is available (though Piñon Flat is still to come). This chapter is addressed to the data accessibility, -transfer and online visualization of the ring laser recordings.

4.1. Datasets from the ring laser observatories

The ring laser laboratories in Christchurch (New Zealand), Wettzell (Germany) and Piñon Flat (USA) provide us with the possibility of detecting the rotational component(s) of ground motion. As the development of this technology to today's instruments, with a very high sensitivity and running stability took two decades, there are major differences concerning data formats, acquisition and accessibility at the testing facilities. In order to visualize these varieties, the data sets of each of the observatories mentioned above is discussed here in detail.

4.1.1. Data from the Christchurch observatory

The observatory in Christchurch was the first facility carrying out the relevant observations, at the beginning mainly focused on physical properties of the instruments. As shown in section 3.2.3 on page 34, the data acquisition at this laboratory is parallely carried out by the local (LabView coded) logging programme on a McIntosh system and via a 'Reftek' data logger.

The LabView data logger

The LabView coded logging programme implemented on a acquisition computer at the Cashmere Cavern is designed to record data files only in the case of an event. A buffer system records 30 minutes of data (starting on the hour or on the half-hour respectively) and stores this 1800 seconds of data as 'eventfile', if the storage process is triggered within this time window. A typical file is composed of
- a header with a size of 88 bytes,
- a datablock containing seven channels of information:
  time, three channels of translation, 'UG-I', 'C-II' and 'G-0' data. At a sample size of 2 bytes the size accumulates to 25000000 bytes (at a sampling rate of 1000 Hz) or 20160000 bytes (at a sampling rate of 800 Hz), respectively and
- a tailer with a size of 64 bytes.

It is stored in a binary format ('EARSS'). A LabView coded processing tool, facilitated the conversion from binary to ASCII format, the downsampling from 800Hz/1000Hz to a standard of 20Hz and a new naming convention:

> 'yyyy-ddd-sssss.dat' containing the data and
> 'yyyy-ddd-sssss.inf' containing the header and tailer information

whereas 'y' is the 'year', 'd' is the 'day of year' and 's' is the sidereal day. The eventdata is stored locally on a harddisk and later on DVDs due to the lack of an internet connection. This recording system has various disadvantages for seismological applications:

- Two successive eventfiles of 1800 seconds length show a gap of up to 8 seconds length in between, as the logging programme finishes the first file before starting the next one. In these 8 seconds no data is available.

- Although a GPS reference frequency is applied for the sampling rate of 1000 Hz, the time stamping of the recorded data relies on the internal computer clock of the McIntosh system.

- During the storage process, the data is not accessible.

The Reftek data logger

The disadvantages of the LabView data logging are compensated since early 2008 by a second acquisition technique employed in Christchurch - a 'Reftek 130' data logger and digitizer. The combination with a SeedLink server/software, which is standard in seismology, allows a continuous data recording, transfer and storage in the miniSeed format. The resulting datafiles, sampled at 20 Hz are stored on the server at the seismological observatory in Fürstenfeldbruck, with the standard nomenclature for miniSeed data:

'NN.SSSSSS..CCC.D.yyyy.ddd'

with 'N' meaning the network name (2 letters), 'S' the station name (up to 6 letters, 'C' the channel name (3 letters), 'D' the 'data', 'y' being the 'year', and 'd' being the 'day of year'. Since February 2008, the near real time rotation data from 'G-0' and 'C-II' can be found on the website: http://www.rotational-seismology.org/data. This data will soon be available for download in the miniSeed format on the online portal http://www.webdc.eu. The recordings of the collocated seismometer can be found on the 'GNS' website at 'http://www.gns.cri.nz'.

4.1.2. Data from the Wettzell observatory

Since its installation in 2001, the recordings from the 'G' ring laser are stored locally on the network of the Fundamentalstation Wettzell. As shown in figure 3.4 on page 26, the data is stored using different sampling rates: 3 seconds (30 seconds), 5 Hz and 20 Hz. The latter value is used as standard sampling rate in seismology. The sagnac frequency estimation for this dataset is carried out by the 'FMD' (frequency demodulator). The recordings from Wettzell were used in several studies and showed a most excellent fit when compared to transverse accelerations (see Igel et al. (2007)). However, this data acquisition and storage system was not designed for real time data access and online visualization.

Since March 2007 the same technique as previously described in section 4.1.1 is applied at the observatory in Wettzell. The combination of a Reftek data logger and the SeedLink/ArcLink software permits a data transfer and storage in the miniSeed format and near real time online visualization of the recorded data at the IWGoRS website: http://www.rotational-seismology.org/data. Since mid 2007 the data from this gyroscope is available for download at http://www.webdc.eu.

4.1.3. Digital and analogue demodulation

As shown in the previous section, the data acquisition at the laboratories in Christchurch and Wettzell is carried out simultaneously by analogue and digital demodulation. The analogue frequency demodulation is carried out by the FMD (frequency demodulator). The digital demodulation is implemented (as additional plug-in) in the SeedLink software, which is used for the data transfer. Both systems realize a sampling frequency of 20 Hz.

In figure 4.2 datasets for two events, (teleseismic and regional) are displayed. The top traces (marked black) on each plot show the rotational motion with analogue demodulation. The traces in the middle section (marked red) display the same time range facilitated with digital demodulation. Both signals are displayed unfiltered. The bottom traces displays the lowpass filtered data with a cutoff period of T = 20 seconds (top event) and T = 10 seconds (bottom event) respectively.

The superior quality of the digital demodulation is clearly visible in both plots. The extraction of a comparable signal from the analogue demodulation demands additional processing of the data and still shows a higher noise level and less accurate results. The traces derived from digital demodulation show a periodic signature of peaks can be seen over the 24 hour rotational seismogram, caused by a problem in the data acquisition, which has now been solved.
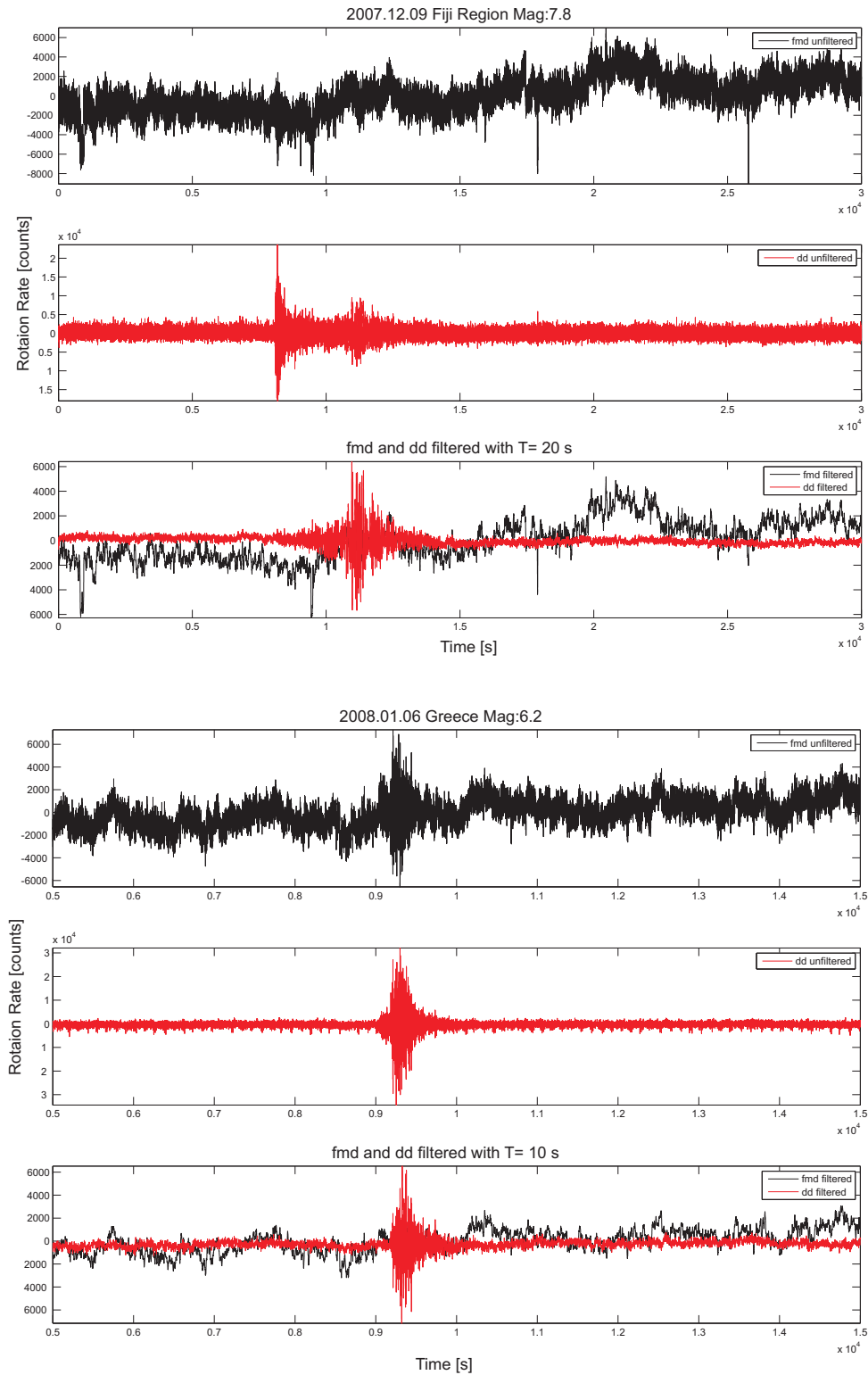
Figure 4.2.: Rotational seismogram for the Fiji event on 9th December of 2007 (Mag 7.8, top) and the Greece event on 6th January of 2008 (Mag 6.2, bottom). The traces are recorded by FMD (top, black, unfiltered), digital demodulation by the 'sagnac plug-in' (middle, red, unfiltered) and the comparison of both signal (bottom, filtered) for the same time range.

4.1.4. Data from the Piñon Flat observatory

The GEOsensor is the latest addition to the ring laser network. It was primarily designed as a modular re-deployable instrument to strike the balance between sensitivity and cost. The datafiles, created by the LabView coded logging unit, hold the three components of translation, two components of tilt, and one component of rotation (with a simultaneous storage of the 'AR(2)' and 'FMD' frequency estimation (see table 4.1.4)). The created files are in the IEEE 754 binary format, the file size is 110592776 byte, with a header of 776 byte at a sampling rate of 20Hz. Each sample has a size of 8 byte (double precision) and each file contains 8 channels of data:

Table 4.1.: Structure of a PFO data file.

channel 1:	time	[s]
channel 2:	seismometer channel E-W	[V]
channel 3:	seismometer channel N-S	[V]
channel 4:	seismometer channel Z	[V]
channel 5:	ring laser rotation rate Z (from FMD)	[V]
channel 6:	tiltmeter N-S	[rad]
channel 7:	tiltmeter E-W	[rad]
channel 8:	ring laser rotation rate Z (from AR2)	[Hz]

These recorded datafiles show a time window of 24 hours and are stored locally on the harddrive of the PXI acquisition unit at the laboratory. The nomenclature of the original datafiles is:

$$GS\_yyyy\_ddd.bin$$

Where 'GS' stands for GEOsensor, 'y' is the 'year' and 'd' is the 'day of year'. As shown in figure 3.17 on page 41, online access for the recorded data is possible via the 'Mercali' server of 'Roadnet'-network of the University of San Diego, California. The script that automates the daily data download of the binary files and converts these datasets into the miniSeed format - which is used as standard in seismology - was developed during this thesis. After the conversion to miniSeed, the file naming is adapted to the standard nomenclature in seismology. A real time data flow and online visualization is not possible using these datasets, as the 24 hour files cannot be accessed until the full volume is stored.

4.1.5. Problems and solutions in data acquisition

At the very beginning of this thesis the emphasis was laid on gathering data from all ring lasers and visualizing the corresponding rotational seismograms in realtime online. This turned out to be a lot more complicated than it appeared at first, as the access to the data from the three stations was not simple.

Due to a change in staff at the SCRIPPS observatory and bad documentation we were not able to obtain an access password for the existing real time capable data transfer system already installed at the Piñon Flat observatory. Although the data is stored locally in a binary format as well, a loss of data in the end of 2006 and the beginning of 2007 occurred, as the harddisk of the acquisition computer has a limited volume of 20 GB and overrides the previous data successively. The only other opportunity to get hold of the data was via the 'Mercali' server of the 'Roadnet'-system. It was not possible to establish a new account on that server, however Dr. A. Velikoseltsev provided his existing account and password for this purpose. This offered the basis for the daily download accomplished by two shell-scripts developed during this study. However, the provided data still needs to be converted to the miniSeed format.

As mentioned before, 'G' was not designed to record seismic signals on a large scale at the beginning. Sampling rates of 3 seconds, 5 Hz and 20 Hz were applied to the raw data and stored on a server in Wettzell, which still is not accessible over the internet. However, the rotational seismograms were displayed of the hompage: http://www.wettzell.ifag.de/. The 20 Hz data, which is of special interest to seismology was sampled by the frequency demodulator, which is an analogue device causing sometimes very high noise levels. In March 2007 a standard seismological acquisition equipment was installed at the station, which allows a transfer of the ring lasers data in near real time and in the miniSeed format.

The data of the active ring laser gyroscopes at Christchurch is stored in a non-standard data format (binary, 'EARSS') at the local acquisition unit. Due to limited harddrive capacity, the data is transferred to DVDs. The time stamping of the recorded data is provided by an internal computer clock, leading to significant drifts in the timing system. This system is still not accessible from outside at all, so older data (before early 2008) can not be downloaded and processed yet. Therefore the same data logger/digitizer unit as in Wettzell was installed here in early 2008, providing online accessibility and GPS time stamping, near real time data access and a data transfer in the miniSeed

format. However, the largest of the Canterbury ring lasers cannot be sampled by the standard digitizer, due to the very high sagnac frequency of approx. 2177 Hz and the comparable small maximum sampling rate of 1000 Hz and the corresponding problems associated with the Nyquist theorem.

4.2. Online visualization and data conversion

This section provides detailed information about the scripts coded to solve the problems of data download, data conversion and online visualization. This was achieved by combining different programming languages.

4.2.1. Coding of shell scripts

Shell script programming is commonly used for the automatisation of command line based processes, with a similarity to programming languages. In this thesis, it was applied to enable a daily download of the data from the Piñon Flat observatory. Each of these datafiles covers a time range of 24 hours (starting at 0.00 UTC) and is available approximately one hour after the data storing is complete. They are stored on the harddrive of the acquisition unit, which is accessible over a ftp connection from the 'Mercali' webserver. In order to accomplish the download of these datasets automatically, six main steps are required described by figure 4.3. These are executed by the shellscript 'pfo2.sh' (1)-(3) and 'pilsen.sh' (4)-(6):

(1):   opening a ftp connection to the PXI-computer,
(2):   download of the latest datafile,
(3):   storing the latest data file on the mercali server,
(4):   opening a connection from a local computer or webserver to the mercali server,
(5):   local storage of the dataset,
(6):   removing the dataset from the mercali server.

Several ideas were reviewed to efficiently automate this file transfer:

- A perl-coded script was developed in collaboration with Dr. Alexander Neidhart at the Fundamentalstation Wettzell. Even though the program was working, it was not possible to run the script on the 'Mercali' server.
- The implementation of a single script executed on a local computer was technically
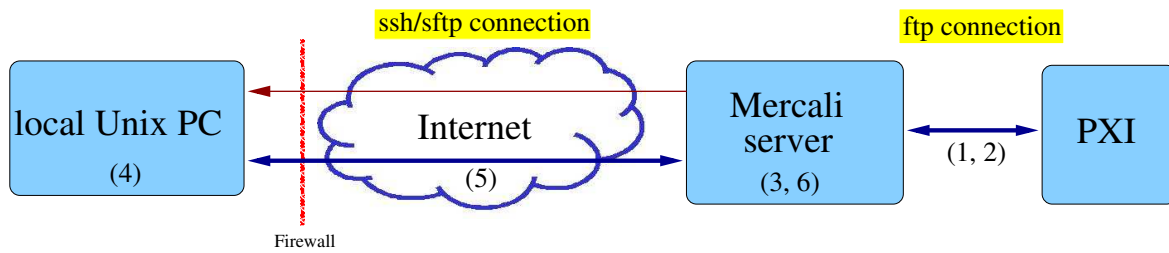
Figure 4.3.: Schematics of the datatransfer between the Piñon Flat observatory and a
local server.

  feasible, however, after the establishment of a connection to the 'Mercali' server an
  access to the data on the PXI computer via ftp is not feasible
- The implementation of a single script stored and executed on the 'Mercali' server
  turned out to have several disadvantages as the passwords for the PXI computer
  (for download) and the password for a server or local computer (for datatransfer) are
  embedded in this program and therefore stored on the 'Mercali' server.

As a result, two scripts were coded in order to guarantee the download. The first script
(called 'pfo2.sh', see A.3 on page 77) is installed on the 'Mercali' server and executed
by a cronjob once every 24h: A ftp connection is opened, username and password are
transmitted, the latest data filename estimated and file downloaded and stored on the
'Mercali' server. After this the ftp connection is closed. This download and storage
process takes up to four hours time.
With respect to this timing interval, the second script (called 'pilsen2.sh', see A.3 on
page 77), installed at a local computer/server, is executed once every 24h. A sftp
connection to the 'Mercali' server is opened, the latest data filename estimated and
the file downloaded and stored on the local server. The download process usually takes
up to 15 minutes. After that, the current file is deleted from the 'Mercali' server to
save storage space. The execution of the python coded data conversion script (bin to
miniSeed, explained in section 4.2.2) is implemented in this shell script. The current
data files are downloaded from the Piñon Flat observatory and automatically converted
to the 'miniSeed' format.

4.2.2. Coding of python scripts

Python is an object-orientated programming language which aims at readability of the
code. This language was used in this study as it is well suited for working with binary
data. It has been stated already that the binary data delivered by the GEOsensor

has to be converted into a standard format for seismology. Here the Seed/miniSeed format was chosen - which is used by IRIS and ORFEUS[1] - as the data from the Christchurch and Wettzell observatories is transferred and stored in this format as well. This program called 'bin2mseed.py' (see appendix A.2 on page 73) converts the binary data in two steps:

(1): from binary to GSE(2.1) (see figure 4.4 steps (2) and (4))
(2): from GSE(2.1) to miniSeed (see figure 4.4 steps (5) and (6)).

As a format converter from GSE(2.1) to miniSeed was available for download and implementation at Orfeus (2008), the coding mainly focused on the binary to GSE(2.1) conversion of the waveforms data. The GSE data format, commonly used in seismology for data storage and data exchange via ftp or Email, has typical structure consisting of 4 sections:

(1): 'WID2' header line (waveform identification)
(2): 'STA2' line (station information)
(3): 'DAT2' block (waveform information)
(4): 'CHK2' block (checksum)

This predefined structure continues in the section as well, with a special emphasis on the correct length and amount of letters and numbers. The parts (1) to (4) are explained in detail in the following paragraphs.

Information given in the WID2 line format (defined in appendix B.1 on page 80) is amongst others general information like 'start date' and 'start time' of the datafile (here the start time is always set to '00:00:00.000', as the recording of a 24 hour datafile starts at midnight UTC). As it can be seen in listing 4.1 on page 53, the station code consists of up to five letters and was stated 'GEOS' for the ring laser component of the GEOsensor. The next information given in the header is the 'FDSN[2]' (international federation of digital seismographs networks) channel code (see Appendix B, page 79) which is usually a standard code for the station. As a broadband ring laser has never been used in this context a new FDSN channel code has to be defined as standard within the next Seed/miniSeed release. In this study we used as channel code 'BAZ' standing for broadband (B) tilt (A) around the z-axis (Z) (see table C on page 83). The next information provided, the 'Sub format', gives information on how the current data is stored in the miniSeed file. For this the possibilities are: 'INT' for 'free format

---

[1]Two international data and research centres for seismology: http://www.iris.edu/ and http://www.orfeus-eu.org/

[2]For further information on the FDSN naming convention see http://www.fdsn.org .

integers' as ASCII characters, 'CM6' or 'CM8', denoting compressed data (6- or 8-bit compression) or 'AUT', 'AU6'/'AU8' (with 'AU' standing for authentification, 'T' standing for uncompressed binary integers and '6' or '8' standing for the compression rate in bit).

Listing 4.1: GSE file sample

```
WID2 2008/01/07 00:00:00.000 GEOS   BAZ       INT  1728000    20.000000
    2.4285e+01   1.000 RLAS      0.0  0.0
STA2             33.60900 -116.45530 WGS-84       0.000 0.000
DAT2
10703
10681
...
...

11321
11300
11090
CHK2 83854092
```

In addition to the number of samples and the sampling rate, the calibration factor is provided. In seismology, the seismic output signal is usually recorded in volts and is subsequently digitized and finally converted to counts, offering storage advantages. To obtain the actual groundmotion in nm, a value - the calibration factor - is needed to convert the data from counts. However, the data from Piñon Flat is stored in Volt. In order to create a standard GSE file the information must be available in counts. This conversion was done using the LSBvalue (least significant bit value) which is defined for an n-bit A/D-converter as (Scherbaum, 1996):

$$LSBvalue = \frac{FullScaleVoltage}{2^{n-1}}. \tag{4.1}$$

In our case this leads to:

$$LSBvalue = \frac{10V}{2^{15}} = \frac{10V}{2^{15}} = 0.00030518V. \tag{4.2}$$

In order to get the calibration factor, the LSBvalue has to be divided by 2π:

$$calibration factor = \frac{LSBvalue}{2\pi} \tag{4.3}$$

The resulting value is stored in the header and used to re-convert the data when needed.

Furthermore, the information of the calibration reference period (in seconds) is given. The calibration factor is only applicable within the reference period. The instrument type was defined as 'RLAS', as the corresponding instrumenttype naming convention does not yet have a rotation meter as choice. The last two values given in the header are the horizontal and vertical orientation of the instrument.

The STA2 line gives exact information on the station itself (see table B.3 on page 81): the network identifier (name), latitude and longitude, the reference coordinate system (here we chose the WGS-84), the elevation and emplacement depth.

In the DAT2 data block (see table B.2 on page 81) all numbers are represented as integer, regardless in which of the six sub formats they are stored.

The checksum algorithm is used in the CHK2 block (see table B.4 on page 81). The checksum is calculated from integer values prior to the sub format conversion. It is computed modulo 100.000.000 and stored as 8 digit integer without sign (GSE, 1997) The enforced line length in the GSE(2.1) does not exceed 1024 bytes, the default line length is 132 characters. After the content of the GSE files has been visualized, the next section will focus on the coding of the data converter.

The final program structure of the python script (named 'bin2mseed.py') converting the binary data from the GEOsensor station to the miniSeed data format is presented by the flowchart figure 4.5 on page 57. First the file defined as 'infilename' (nomenclature: 'GS_yyyy_ddd.bin') is opened (1). The information given in the header, which is in the first 776 bytes of the file, is extracted. The size of the samples, the number of samples and the number of channels is calculated. A 'for loop' then creates the GSE file structure (2), which contains general information on the instrument as well as location and time information, as explained in section 4.2.2. Seven GSE files are created, one for each channel of the 'infile'. After the storage of the seven files (4), a for loop employing the gse2mseed converter arranges the conversion of all channels to the miniSeed format (5). Once this process is finished, the filenames of the miniseed files (nomenclature: 'GS_yyyy_ddd.mseed') have to be adapted according to the standard miniSeed naming convention (6). Therefore, the filename is changed automatically to

$$\text{'NN.SSSSSS..CCC.D.yyyy.ddd'}$$
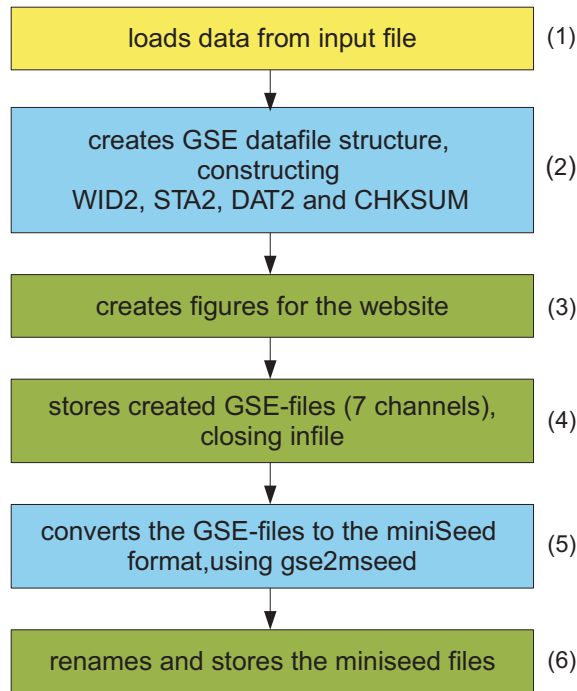
Figure 4.4.: Structure flowchart of the python-coded data converter.

with 'N' being the network name, 'S' the station name, 'C' the channel, 'D' the data, 'y' the year, 'd' the day of year. At last, the miniSeed files are stored to a directory tree, every channel having its own folder. The online visualization (3) of these miniSeed files is included in the python script. A visualization similar to the data from Christchurch and Wettzell is not possible, as the dataflow from Piñon Flat is not in real time. Additionally, there is still a lack of applicable filter values for the data prohibiting a presentable result at the moment. A typical problem for the definition of a standard filter can be seen in figure 2.3 on page 20, where mode hops and split mode operation need to be filtered out, while the earthquake signal still has to be visible. The data is expected to be visible online at the website 'http://www.rotational-seismology.org/data' within early 2008.

4.2.3. Coding of html/php scripts

In order to efficiently visualize the rotational seismograms delivered by the stations 'G' in Wettzell, 'C-II' and 'G-0' in Christchurch, html/php coded scripts needed to be designed. 'HTML' stands for 'hypertext markup language' and is commonly used for programming websites. 'PHP'-code, meaning 'hypertext preprocessor', is often part of 'HTML' scripts. It is a programming language designed for coding dynamic contents.

The implementation of the online visualization asks for two steps: creation of the plots (for all stations and dates) and coding of the script that actually illustrates these plots online. The miniSeed data from Wettzell and Christchurch are transferred in near real time to the 'Earthworm'-system in Fürstenfeldbruck. Latter represents an internet based 'toolkit of processing modules' (Johnson et al., 2008) for seismic data. The miniSeed data is stored in a SQL database, which allows the visualization by using the 'helicorder' plug-in of the 'Winston' wave server. This is a standard tool in seismology for the online visualization e.g. of translations.

The system is adapted for the creation of rotational seismograms and provides a figure subsequently presenting the latest waveform data. These figures show a frame filled with data with a maximum of six hours. Additionally, so called 'event files' are created showing traces of translation and rotations for selected time windows (in case of an earthquake). The according 'event list' is created automatically by checking the data of the Swiss Seismological Service for relevant earthquake information. All figures mentioned above are stored locally at the Seismological Observatory in Fürstenfeldbruck. In figure 4.5 on page 57, the two branches of the program ('Visualization_Wettzell.php') facilitating the online visualization of the miniSeed data from Christchurch and Wettzell are displayed.

The first branch implements the rotational seismograms and allows an online presentation of the plots (see figure 4.6 on page 58), the second branch includes an uptodate earthquake event list (see figure 4.7 on page 59) on the webpage. The most recent rotational seismogram is automatically displayed on the page and updated every five minutes, presenting the waveforms in near real time. On top of this figure dropdown menus are enabling a user to define certain parameters of the figure displayed. These are: 'station', 'year', 'month', 'day' and 'time'. By selecting the 'go'-button, the php-script checks, whether or not a datafile according to the parameters exists (see figure 4.5 on page 57). 'No data available' is displayed on the website, if no (current or requested) dataset for these variables is stored.

Beneath the seismograms an 'eventlist' is displayed, obtaining its information from the earthquake list mentioned above. The latest events, numbered in ascending order, are selectable by a link in the list (see figure 4.7 on page 59). When an event is selected, a new window opens, displaying the translational (as acceleration) and rotational data for the selected event. This display is realized by the implementation of a script called 'vs.php' (see script A.1 on page 70), which creates a new window and displays supplementary information, and a script called 'turn.php' (see script A.1 on page 71) which rotates the figure into a horizontal position.
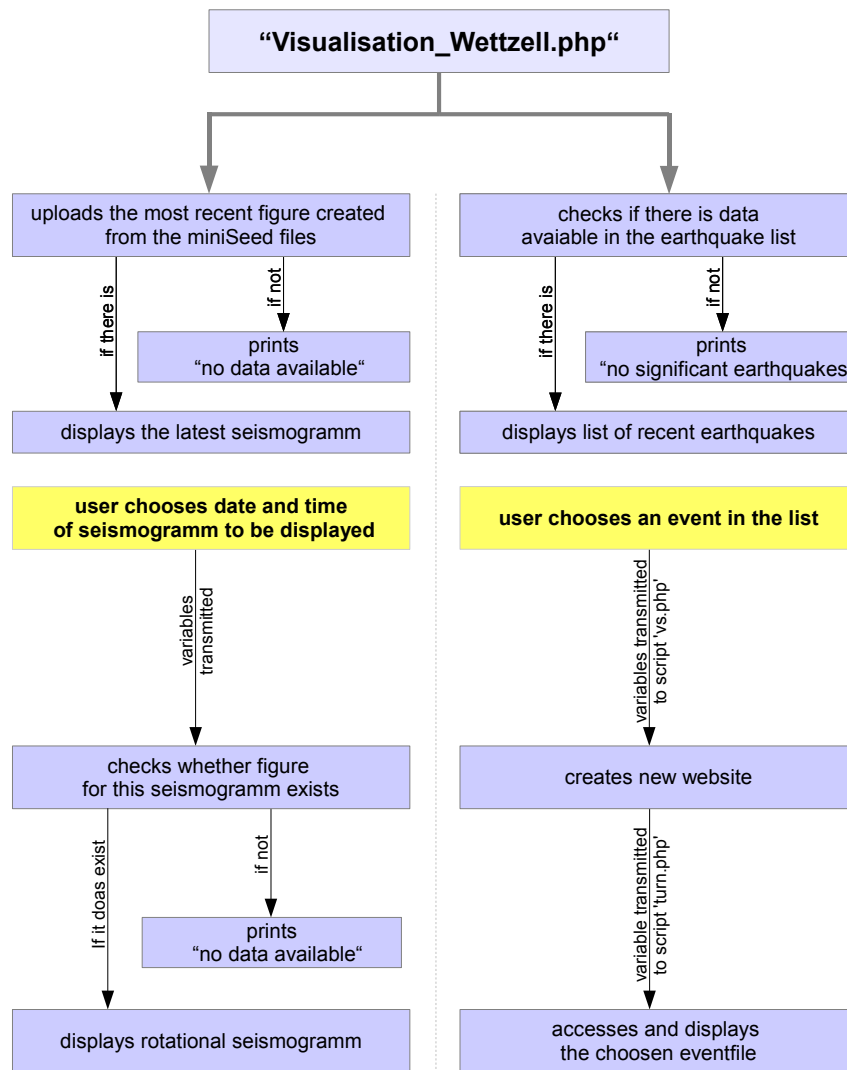
Figure 4.5.: Flowchart describing the two branches of the implemented html/php scripts designed for visualization of the real time data recorded at the observatories in Wettzell and Christchurch.

This eventlist is available for the Wettzell ring laser only, as the establishment of an automated system displaying the figures of translations and rotations for Christchurch has not been implemented yet. Please note, that data for the rotational seismograms is available starting at: March 12th, 2007 for Wettzell and Feb. 27th, 2008 for the Christchurch stations. Additionally to the eventlist, an archive is going to present data from older events quite in the same way. However, this function is still to come.

4.3. Online presentation

An important goal achieved in this thesis is the first ever online visualization of ring laser instruments. Figure 4.6 shows a screenshot of the 'IWGoRS'-website displaying the continuous near real time data of a time period of six hours. In addition, the onset of the Fiji Islands Mag:7.8 earthquake on the 9th of December, 2007 can be seen. Beneath the rotational seismogram an 'event-list' is displayed (figure 4.7). Here, the information on latest major earthquakes like location, depth and magnitude can be retrieved. Furthermore, several drop-down menus offer the chance to choose the time window and station of interest.

By choosing one of the earthquake included in the 'event-list', a new window (figure 4.8 on page 59) is generated that displays the translational and rotational data in the following form:

- acceleration of the Z-component (black),
- acceleration of the radial component (black),
- acceleration of the transverse component (blue),
- rotational seismogram (red)

This feature offers the possibility to check the similarity in waveform and amplitude of the translational and rotational motions.

Figure 4.6.: This figure shows a screenshot of the website www.rotational-seismology.org.
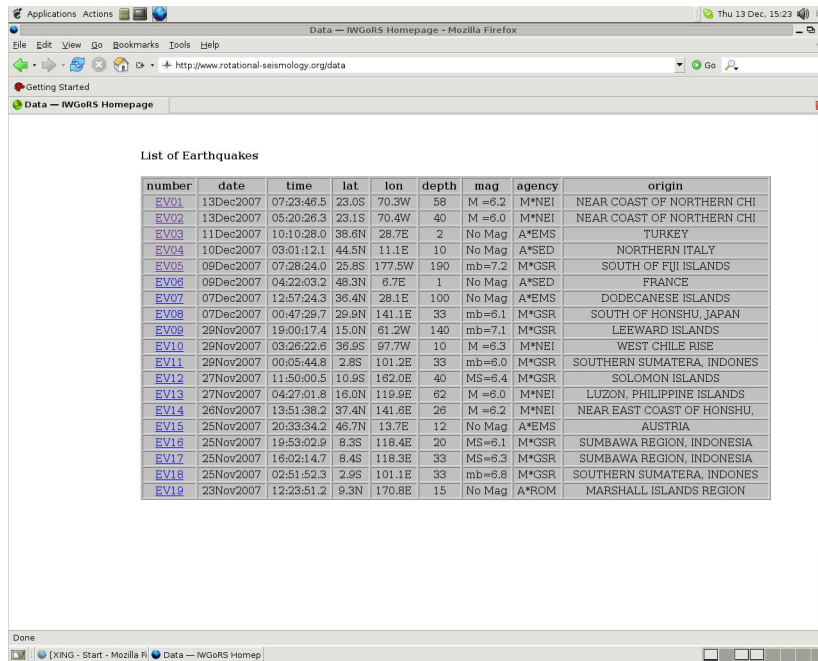
Figure 4.7.: This figure shows a example of the dynamically created earthquake list on the 'IWGoRS'-website.
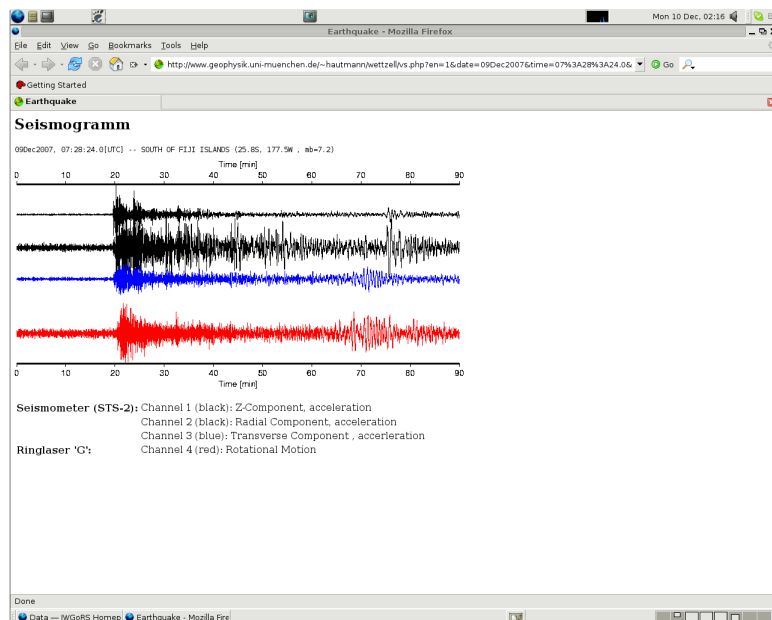
Figure 4.8.: This figure shows a screenshot of the event data, selectable in the event list on the website.

4.4. Conclusion

On the 'IWGoRS'-website the data of three ring laser gyroscopes are presented in near real time. Many different technical problems had to be overcome to realize the online visualization of the data recorded by ring laser gyroscopes. Therefore, we conclude that it is crucial to develop standards for data acquisition data transfer and data formats in order to ease future projects and enable ring laser data networks. Despite an excellent running stability, it was not possible until today, to record an earthquake on all three ring laser locations.

Chapter 5.

Conclusion and Discussion

This thesis provides the foundation for standard procedures in data acquisition, transfer and online visualization of ring laser measurements. Here we present these processes for the ring laser gyroscopes situated at the observatories in Christchurch (New Zealand), Wettzell (Germany) and Piñon Flat (USA) in detail. As the evolution of the relevant instruments took place over a long period of time and the sensors were initially not designed for seismological applications, differences in data acquisition methods, data storage systems, data formats and accessibility of the records had to be overcome in order to guarantee a near real time online visualization of the gyroscopes data in a standardized format. Each ring laser observatory facilitates different technical features according to the intended field of application at the time of deployment.

At the laboratory in Christchurch there are currently two ring laser gyroscopes recording rotational motions around the vertical axis and one instrument providing measurements around a horizontal axis of rotation. Since the inauguration of the facility, the data gathered by the gyroscopes is stored in a binary format (EARSS) on the harddrive of the local acquisition system. The data provided by this system was not available for download and therefore stored on DVDs. Since early 2008 an additional logging system offers near real time data acquisition. The involved Reftek digitizer/data logger enables, in collaboration with the SeedLink/ArcLink software, access to the data recorded by two ('G-0','C-II') of the three ring lasers and allows storage of the data in the standard miniSeed format and online visualization on the website http://www.rotational-seismology.org. A php-coded program was developed during this thesis enabling a near real time online visualization of this data.

The ring laser ('G') at the Wettzell observatory is operable since the end of 2001. This gyroscope is the most sensitive large perimeter rotation sensor worldwide. Its data

is stored in the ASCII data format at the server of the Fundamentalstation Wettzell with three different sampling rates: 3 seconds, 5 Hz and 20 Hz. The recorded data is not accessible via the internet and the sagnac frequency estimation of the 20 Hz data, which is of major interest in seismology, is not very accurate. Similar to Christchurch, a secondary data acquisition system for geophysical research was installed, employing a Reftek data logger and the SeedLink/ArcLink software. A sampling rate of 20 Hz is applied and a digital demodulation of the recorded data results in an excellent data quality and signal/noise ratio. This data is stored in the miniSeed format, visualized online in the same way as the Christchurch data and is available for download at http://www.webdc.eu.

At the end of 2005 the only rotation sensor primary planned and designed for geophysical applications, the 'GEOsensor' had been installed at the Piñon Flat observatory. This system consists of a ring laser gyroscope, a standard three axis seismometer, a GPS time and frequency reference and a tiltmeter. The data recorded at this observatory is stored locally on the harddisk of the acquisition computer in a binary format with a sampling rate of 20 Hz. Each datafile contains 24 hours of information from three translational components, two tiltmeter components and two rotational components (FMD and AR(2) frequency estimation). At the laboratory a Quanterra q330 datalogger/digitizer is installed providing the possibility of near real time data acquisition. However, this datalogger device can still not be enabled. Momentarily, the data can not be accessed during the storing process prohibiting a near real time online visualization.

In the course of this thesis the online visualization of three ring laser gyroscopes ('G','G-0','C-II') was established by coding and implementation of several scripts (python/php/shell). The daily download of the GEOsensor data and a conversion of these files into the miniSeed format has be achieved. The online visualization of the data from Piñon Flat is still in progress as adequate filter settings for the rotational seismograms must be found first. Although various earthquakes have been recorded at the three ring laser locations, there is not a single event recorded by all three instruments. A significant improvement in signal quality of the digitally demodulated data can be reported. Before the ring laser recordings will become available in the miniSeed format at e.g. the WebDC data portal, a naming convention for the rotational data with the Seed/miniSeed release must be defined. We therefore propose the employment of Reftek data loggers and the SeedLink/ArcLink software as standard for future ring laser laboratories due to the real time capability, standard sampling rate, standard data format and extraordinary signal quality of the system.

Appendix A.

Programs

A.1. html/php

Listing A.1: Php-coded script for the online visualization of near real time miniSeed data from the ring laser observatories Wettzell (Germany) and Christchurch (New Zealand)

```php
1  <?php
2
3    header( 'refresh: 300; url='.$_SERVER['PHP_SELF']);
4
5    $KORREKTUR = -2*60*60;
6
7    $STATIONS = array('BRLAS','BNZG0','BNZC2');
8
9
10   $timestamp = time();
11   $timestamp = $timestamp-(2*60*60);
12 ?>
13 <html>
14 <head>
15 <body>
16
17 <form action="" method="get">
18   <?php
19
20     $station = $STATIONS[0];
21     if (@$_GET['timestamp'])
22     {
23         $timestamp = intval($_GET['timestamp']);
24
25     }
26     if (@$_GET['button'])
27     {
28         $button = $_GET['button'];
29         if ($button == 'Now') e
30         {
31             $timestamp = time();
32             $timestamp = $timestamp + $KORREKTUR;
33             $station = $_GET['station'];
34         }
35         else if ($button == 'Next')
36         {
37             $timestamp += 6*60*60;
38             $station = $_GET['station'];
39
```

```
40              }
41          else if ($button == 'Prev')
42          {
43              $timestamp -= 6*60*60;
44              $station = $_GET['station'];
45
46          }
47          else if ($button == 'Go')
48          {
49              $month = $_GET['month'];
50              $year = $_GET['year'];
51              $day = $_GET['day'];
52              $hour = $_GET['hour'];
53              $station = $_GET['station'];
54              $timestamp = mktime($hour+2,0,0,$month,$day,$year)
55              + $KORREKTUR;
56          }
57      }
58      $datum = getDate($timestamp);
59      $year = $datum['year'];
60      $month = $datum['mon'];
61      $day = $datum['mday'];
62      $hour = $datum['hours'];
63
64 ?>
65    <br />
66    <input type="hidden" name="timestamp" value=
67    "<?php echo $timestamp; ?>" />
68    <input type="submit" name="button" value="Prev" />
69    <input type="submit" name="button" value="Next" />
70       
71    <input type="submit" name="button" value="Now" />
72
73       
74    station:
75    <select name="station">
76 <?
77      foreach ($STATIONS as $value)
78      {
79        echo '<option value="'.$value.'"';
80        if ($value==$station)
81        {
82          echo ' selected="selected"';
83        }
84        echo '>'.$value.'</option>';
85      }
```

```
 86 ?>
 87   </select>
 88
 89   year:
 90   <select name="year">
 91 <?php
 92   for ($i=2007;$i<=2008;$i++)
 93 {
 94   echo '    <option value="'.$i.'"';
 95   if ($i==$year)
 96   echo ' selected="selected"';
 97   echo '>'.$i.'</option>'."\n";
 98 }
 99 ?>
100
101   </select>
102   month: <select name="month">
103
104 <?php
105   for ($i=1;$i<=12;$i++)
106 {
107   echo '    <option value="'.$i.'"';
108   if ($i==$month)
109   echo ' selected="selected"';
110   echo '>'.$i.'</option>'."\n";
111 }
112 ?>
113
114   </select>
115   day: <select name="day">
116
117 <?php
118
119   for ($l=1;$l<=31;$l++)
120 {
121   echo '    <option value="'.$l.'"';
122   if ($l==$day)
123   echo ' selected="selected"';
124   echo '>'.$l.'</option>'."\n";
125 }
126
127 ?>
128
129   </select>
130   hour: <select name="hour">
131
```

```
132  <?php
133
134    for ($h=0;$h<=23;$h++)
135  {
136    echo '     <option value="'.$h.'"';
137    if ($h==$hour)
138    echo ' selected="selected"';
139    echo '>'.$h.'</option>'."\n";
140  }
141
142  ?>
143
144    </select>
145    <br>      
146           
147           
148           
149           
150       
151    <input type="submit" name="button" value="Go"
152         style="width:570; height:25;"/>
153  </form>
154
155  <?php
156
157    if ($hour<6)
158      $part = 0;
159    else if ($hour<12)
160      $part=6;
161    else if ($hour<18)
162      $part=12;
163    else
164      $part=18;
165
166
167    $imageurl =
168     sprintf('http://observatory.geophysik.uni-muenchen.de/
169                      seismology/wettzell/WWWGifs/
170                      %5s_%02d%02d%02d_%02d.gif',
171          $station,$station,$day,$month,
172          substr($year,2),$part);
173
174    $urlhandler = @fopen ($imageurl,"r");
175    if ($urlhandler)
176    {
177      echo '<img src="'.$imageurl.'" alt="" />';
```

```php
178      fclose($urlhandler);
179    }
180    else
181    {
182      print "No data available";
183    }
184
185
186 ?><br><br><br>
187
188    <h4>List of earthquakes for the 'G' ring laser Wettzell/Germany</h4>
189
190 <?php
191
192 $lines = file('http://observatory.geophysik.uni-muenchen.de/
193              seismology/wettzell/EV/sed-manual.txt');
194
195    if (count($lines)==1 && $lines[0][0]!="E")
196 {
197   echo "---no significant earthquakes recorded in the last 24h---";
198 }
199
200 else
201
202 {
203 ?>
204   <table align="left" border="1" width="100%" bgcolor="#C0C0C0">
205     <tr>
206      <th>number</th>
207      <th>date</th>
208       <th>time</th>
209      <th>lat</th>
210      <th>lon</th>
211      <th>depth</th>
212      <th>mag</th>
213      <th>agency</th>
214      <th>origin</th>
215
216   </tr>
217
218 <?php
219 $lines = file('http://observatory.geophysik.uni-muenchen.de/
220              seismology/wettzell/EV/sed-manual.txt');
221 $uniquelines = array();
222 $newlines = array();
223
```

```php
224 for ($i=0; $i<count($lines); $i++)
225 {
226     $line = $lines[$i];
227     $temp = substr($line, 4);
228     if (!array_search($temp, $uniquelines))
229     {
230       $uniquelines[]=$temp;
231     }
232 }
233
234 for ($i=0; $i<count($newlines); $i++)
235
236 {
237     $arr=explode(' ',$newlines[$i]);
238
239       $j = $i + 1;
240       if ($j<10)
241       {
242       $h = sprintf("0%s",$j);
243       }
244       else
245       {
246       $h = $j;
247       }
248
249     $nr = sprintf("EV%s",$h);
250     $date = $arr[3];
251     $time = $arr[4];
252     $temp = array_slice($arr, 5);
253     $hinten = implode(' ',$temp);
254
255
256     $lat = trim(substr($hinten, 0, 5));
257     $lng = trim(substr($hinten, 6, 6));
258     $depth = trim(substr($hinten, 12, 3));
259     $mag = trim(substr($hinten, 16, 6));
260     $station = trim(substr($hinten, 23, 5));
261     $loc = trim(substr($hinten, 29));
262
263
264     $url =
265     sprintf('vs.php?en=%d&date=%s&time=%s&origin=%s&
266             lat=%s&lon=%s&mag=%s',urlencode(substr($arr[0],2)),
267             urlencode($date),urlencode($time),urlencode($loc),
268             urlencode($lat),urlencode($lng),urlencode($mag));
269
```

```
270    echo "<tr align= center >";

271

272     echo "<td>", "<a href= $url target= _blanc >".  $nr."</a>", "</td>";
273     echo "<td>".  $date."</td>";
274     echo "<td>".  $time."</td>";
275     echo "<td>".  $lat."</td>";
276     echo "<td>".  $lng."</td>";
277     echo "<td>".  $depth."</td>";
278     echo "<td>".  $mag."</td>";
279     echo "<td>".  $station."</td>";
280     echo "<td>".  $loc."</td>";

281

282    echo "</tr>";

283

284

285 }
286 }
287 ?>
288 </table>
289 </body>
290 </html>
```

Listing A.2: Php-coded script for the display of eventdata on the 'IWGoRS'-website

```
1  $seis = "Seismogramm";
2  if (@$_GET['en'])
3  {
4     $en = strval($_GET['en']);
5  }
6  if (@$_GET['date'])
7  {
8     $date = strval($_GET['date']);
9  }
10 if (@$_GET['time'])
11 {
12    $time = strval($_GET['time']);
13 }
14 if (@$_GET['origin'])
15 {
16    $origin = strval($_GET['origin']);
17 }
18 if (@$_GET['lat'])
19 {
20    $lat = strval($_GET['lat']);
21 }
22 if (@$_GET['lon'])
23 {
```

```
24    $lon = strval($_GET['lon']);
25 }
26 if (@$_GET['mag'])
27 {
28    $mag = strval($_GET['mag']);
29 }
30
31 echo "   <h2>". $seis."</h2>\n";
32 echo "   <pre>". $date,",","  ", $time,"[UTC]"," ","--",
33            " ","$origin"," ","(", "$lat", ",", " ",
34            "$lon"," ,", " ", "$mag",")"."</pre>\n";
35 ?>
36 <img src="turn.php?en=<?php echo $en; ?>" /><br><br>-->
37 <table>
38    <tr>
39       <td><b>Seismometer (STS-2):</b></td>
40       <td>Channel 1 (black): Z-Component, acceleration</td>
41    </tr>
42    <tr>
43    <td></td>
44       <td>Channel 2 (black): Radial Component, acceleration</td>
45    </tr>
46    <tr>
47       <td></td>
48       <td>Channel 3 (blue): Transverse Component , accerleration</td>
49    </tr>
50    <tr>
51       <td><b>Ringlaser 'G':</b></td>
52       <td>Channel 4 (red): Rotational Motion</td>
53    </tr>
54 </table>
55 </body>
56 </html>
```

Listing A.3: Php-coded script adapting event figures for the 'IWGoRS'-website

```
1 <?php
2
3 function rotate($source)
4 {
5   $w = imagesx($source);
6   $h = imagesy($source);
7   $rotate = ImageCreate($h,$w);
8   imagepalettecopy($rotate,$source);
9   ImageCopyResized($rotate, $source, 0, 0, 0, 0, $h, $w, $w, $h);
10   for ($x=0;$x<$w;$x++)
11   {
```

```php
12       for ($y=0;$y<$h;$y++)
13       {
14         $color = imagecolorat($source, $x, $y);
15         imagesetpixel($rotate, $h-$y-1, $x, $color);
16       }
17    }
18    return $rotate;
19 }
20 if (@$_GET['en'])
21 {
22    $en = intval($_GET['en']);
23 }
24 else
25 {
26    $en = 1;
27 }
28
29
30 $pic =  sprintf('http://observatory.geophysik.uni-muenchen.de/
31                 seismology/wettzell/EV/EV%1d.gif',$en);
32
33 $degrees = 90;
34
35 header("Content-type: image/gif");
36
37
38 $source = imagecreatefromgif($pic);
39 $rotate = rotate($source);
40
41 imagegif($rotate);
42 ?>
```

A.2. Python

Listing A.4: Python-coded binary to miniseed converter

```python
#!/usr/bin/env python
# -*- coding: utf-8 -*-

import sys, struct, time, re, os, math
import Image, ImageDraw

insttypes = ['','LE-3D','LE-3D','LE-3D','RLAS','LGM1','LGM2','RLAS']
FDSN_channel = ['tim','BHE','BHN','BHZ','BAZ','BAN','BAE','HAZ']

print "bin2mseed Converter V0.8"

try:
    infilename = sys.argv[1]
    gsefilename = infilename.split('.')[0]+'.%3s.gse'
except:
    print "Usage: " + sys.argv[0] + " filename.bin"
    sys.exit(1)

ifile = open(infilename, 'rb')

print "Reading from " +infilename+ " ..."


header={}
data = ifile.read(776)
header['rate'] = data[746:751]
header['channels'] = data[774:776]
header['starttime'] = data[726:734]
header['date'] = data[705:713]

data = ifile.read()
datalen = len(data)

samplesize = struct.calcsize('d')
channels = int(header['channels'])
chunklen = channels*samplesize
chunks = int(datalen/chunklen)
samples = chunks*channels

d = re.compile('(\.)')
date = d.sub('/', header['date'])
time = header['starttime']
```

```python
43  stime = time+".000"
44
45  outdata = struct.unpack('>'+'d'*samples,data)
46
47  for channel in range(1,channels,1):
48
49      station = "GEOS"
50      auxid = ''
51      samprate = 20
52      lsb = 10/math.pow(2,16)
53      calib = (lsb/(2*math.pi))*math.pow(10,6)
54      calper = 1
55      hang = 0
56      vang = 0
57      format = 'INT'
58
59      gsefile = gsefilename % FDSN_channel[channel]
60      ofile = open(gsefile, 'w')
61
62      ofile.write("WID2 20%-8s %-12s %-5s %-3s %-4s %-3s
63                  %8i %11.6f %10.4e %7.3f %-6s %5.1f %4.1f\n" % \
64                  (date,stime,station,FDSN_channel[channel],auxid,
65                  format,chunks,samprate,calib,calper,
66                  insttypes[channel],hang,vang)  )
67
68      network = ''
69      lat = 33.6090
70      lon = -116.4553
71      coordsys = 'WGS-84'
72      elev = 0
73      edepth = 0
74      ofile.write("STA2 %-10s %9.5f %10.5f %-12s %5.3f %5.3f\n" %
75                  (network,lat,lon,coordsys,elev,edepth))
76
77      # DAT2
78      ofile.write("DAT2"+os.linesep)
79
80      MODULO_VALUE = 100000000
81
82      checksum = 0
83      bilddata = []
84      for i in range(channel, len(outdata),channels):
85          valued = outdata[i]
86          value = int(valued/lsb + 0.5)
87          if channel==4:
88              bilddata.append(value)
```

```
 89        ofile.write(repr(value))
 90        ofile.write(os.linesep)
 91
 92
 93        if abs(value) >= MODULO_VALUE:
 94            value = value - (value/MODULO_VALUE)*MODULO_VALUE
 95        checksum = checksum + value
 96        if abs(checksum) >= MODULO_VALUE:
 97            checksum = checksum - (checksum/MODULO_VALUE)*MODULO_VALUE
 98
 99    temp = "CHK2 %08d" % abs(checksum)
100    ofile.write(temp +os.linesep)
101    ofile.write(os.linesep)
102
103    print "writing to " + gsefile
104
105 )
106    if channel == 4:
107        width = 750
108        height = 400
109        border_x = 65
110        border_y = 50
111        im = Image.new('RGB', (width+2*border_x, height+2*border_y),
112            (255, 255, 255))
113        draw = ImageDraw.Draw(im)
114
115        def drawWiggle(y_offset,samples):
116            l=len(samples)
117    x=border_x
118    y=border_y+y_offset
119            for i in range(0,l,24):
120       subsample=samples[i:i+24]
121            max_y=max(subsample)/5000+y
122     min_y=min(subsample)/5000+y
123            draw.line((x,min_y,x,max_y), fill=128)
124            x=x+1
125        draw.line((border_x,border_y, width+border_x, height+border_y),
126                fill=128)
127        for x in range(0,width,width/15):
128          draw.line((border_x+x,border_y, border_x+x, height+border_y),
129                fill=128)
130        values = bilddata[0:18000]
131        drawWiggle(15,values)
132        im.save("copy.png","PNG")
133
134 ofile.close()
```

```
135 ifile.close()
136
137
138
139 for channel in range(1,channels,1):
140     gsefile = gsefilename % FDSN_channel[channel]
141     temp = "./gse2mseed -r 512 "+gsefile
142     os.system(temp)
143
144     mseedinfile = gsefile.split('.gse')[0]+'.mseed'
145     temp = "BW.GEOS..%3s.D." % FDSN_channel[channel]
146     mseedoutfile = temp+infilename[3:7]+"."+infilename[8:11]
147     temp = "mv "+mseedinfile+" "+mseedoutfile
148     print "renaming "+mseedinfile+" to "+mseedoutfile
149     os.system(temp)
150
151     link1 = '/home/hautmann/Desktop/2007/BW/GEOS/%3s.D' % FDSN_channel[
            channel]
152     temp2 = "mv "+mseedoutfile+" "+link1
153     os.system(temp2)
154
155 os.system("mv *.gse /home/hautmann/Desktop/2007/BW/GEOS/gsefiles2007")
```

Listing A.5: Python-coded multifile converter

```
 1 #!/usr/bin/env python
 2 # -*- coding: utf-8 -*-
 3
 4 import os, glob
 5
 6 print "multifile converter V1.0"
 7
 8 filelist = glob.glob('*.bin')
 9
10 for f in filelist:
11     temp = './bin2mseed.py '+f e
12     os.system(temp)
```

A.3. shell

Listing A.6: Shell-coded download script installed on the 'Mercali'-server

```
1  #!/bin/bash
2
3  dayofyear=`date --date 'yesterday' +'%j'`
4  year=`date --date 'yesterday' +'%Y'`
5
6  filename='GS_'$year'_'$dayofyear'.bin'
7
8  cd /home/AlexV/pfo
9  `wget -q ftp://admin:GEOsensor_PF_2005+@172.23.34.41/data/$filename`
```

Listing A.7: Shell-coded download script installed on a local server/computer implementing the Python-coded binary to miniseed converter (see listing A.2)

```
1   #!/bin/bash
2
3   dayofyear=`date --date 'yesterday' +'%j'`
4   year=`date --date 'yesterday' +'%Y'`
5
6   filename='GS_'$year'_'$dayofyear'.bin'
7
8   # cd /home/hautmann/Desktop/link_to_new
9
10  # echo -e "cd pfo \n get $filename \n rm $filename \n exit" | sftp -b -
        alexv@mercali.ucsd.edu
11
12  ./bin2mseed.py $filename
```

Appendix A. Programs

Appendix B.

GSE file line formats

Table B.1.: WID2 line format for GSE files, see GSE (1997).

Position	Name	Format	Description
1-4	"WID2"	a4	Must be "WID2"
6-15	Date	i4,a1,i2,a1,i2	Date of the first sample (yyyy/mm/dd)
17-28	Time	i2,a1,i2,a1,f6.3	Time of the first sample (hh:mm:ss.sss)
30-34	Station	a5	Station code
36-38	Channel	a3	FDSN channel code
40-43	Auxid	a4	Auxiliary identification code
45-47	Subformat	a3	"INT", "CMn", or "AUx" INT is free format integers as ASCII characters; "CM" denotes compressed data, and n is either 6 (6-bit compression), or 8 (8-bit binary compression) "AU" signifies authentication and x is T (uncompressed binary integers), 6 (6-bit compression), or 8 (8-bit binary compression)
49-56	Samples	i8	Number of samples
58-68	Samprate	f11.6	Data sampling rate (Hz)
70-79	Calib	e10.2	Calibration factor; i.e., the ground motion in nanometers per digital count at calibration period (calper)
81-87	Calper	f7.3	Calibration reference period; i.e., the period in seconds at which 'Calib' is valid; calper should be near the flat part
89-94	Instype	a6	Instrument type (from Table 8)
96-100	Hang	f5.1	Horizontal orientation of sensor, measured in positive degrees clockwise from North (-1.0 if vertical)
102-105	Vang	f4.1	Vertical orientation of sensor, measured in degrees from vertical (90.0 if horizontal)

Table B.2.: DAT2 line format for GSE files, see GSE (1997).

Position	Name	Format	Description
Header Line			
1-4	"DAT2"	a4	Must be "DAT2"
Data Lines			
1 - 1024 (available)	Data	i, a, or f	Data values

Table B.3.: STA2 line format for GSE files, see GSE (1997).

Position	Name	Format	Description
1-4	"STA2"	a4	Must be "STA2"
6-14	Network	a9	Network identifier
16-34	Lat	f9.5	Latitude (degrees, S is negative)
36-45	Lon	f10.5	Longitude (degrees, W is negative)
47-58	Coordsys	a12	Reference coordinate system (e.g., WGS-84)
60-64	Elev	f5.3	Elevation (km)
66-70	Edepth	f5.3	Emplacement depth (km)

Table B.4.: CHK2 line format for GSE files, see GSE (1997).

Position	Name	Format	Description
Checksum Line			
1-4	"CHK2"	a4	Must be "CHK2"
Data Lines			
6 - 13	Checksum	i8	For checksum calculation see GSE (1997)

Appendix C.

FDSN naming conventions

Table C.1.: Channel band codes, see GSE (1997).

Band code	Band type	Sample rate [Hz]	Corner period (seconds)
E	Extremely Short Period	> 80	< 10 sec
S	Short Period	> 10 to < 80	< 10 sec
H	High Broadband	> 80	> 10 sec
B	Broadband	> 10 to < 80	> 10 sec
M	Mid Period	> 1 to < 10	
L	Long Period	= 1	
V	Very Long Period	= 0.1	
U	Ultra Long Period	= 0.01	
R	Extremely Long Period	= 0.001	
W	Weather/Environmental		
X	Experimental		

Table C.2.: Channel orientation codes, see GSE (1997).

Orientation Code	Description
Z, N, or E	Traditional (Vertical, North-South, East-West)
A, B, or C	Triaxial (along the edges of a cube turned up on a corner)
T or R	For Transverse and Radial rotations
1, 2, or 3	Orthogonal components but non traditional orientations
U, V, or W	Optional components
H	Hydrophone
F	Infrasonic pressure
C	Coherent beam
I	Incoherent beam
O	Origin beam

Table C.3.: Channel instrument codes, see GSE (1997).

Instrument Code	Description
H	High Gain Seismometer
L	Low Gain Seismometer
G	Gravimeter/Accelerometer Seismometer
M	Mass Position Seismometer
C	Beamed Trace
D	Pressure Sensor

List of Figures

List of Tables

List of Tables

Bibliography

Aki, K., Richards, P., 2002. Quantitative Seismology. University Science Books.

Bodin, P., Gomberg, J., Singh, S., Santoyo, M., 1997. Dynamic deformation of shallow sediments in the valley of Mexico, part i: Three-dimensional strains and rotations recorded on a seismic array. Bull. Seism. Soc. Am. 87, 528–539.

Bouchon, M. B., Aki, K., 1982. Strain, tilt, and rotation associated with strong ground motion in the vicinity of earthquake faults. BSSA 72, 1717–1738.

C-I, 2008. University of Canterbury, C-I ring laser project, 31.01.2008, http://www.phys.canterbury.ac.nz/research/laser/ring_c1.shtml.

C-II, 2008. Fundamentalstation Wettzell homepage, C-II ring laser project, 31.01.2008, http://www.wettzell.ifag.de/.

Cashmere, 2008. Ring laser locations at the Cashmere Cavern, Christchurch, New Zealand, http://www.ringlaser.org.nz/content/cashmere_cavern_laboratory.php.

Cochard, A., Igel, H., Schuberth, B., Suryanto, W., Velikoseltsev, A., Schreiber, U., Wassermann, J., Scherbaum, F., Vollmer, D., 2006. Rotational motions in seismology: theory, observations, simulation. In: Teisseyre, e. a. (Ed.), Earthquake source asymmetry, structural media and rotation effects. Springer Verlag.

G-0, 2008. University of Canterbury, picture of the G-0 ring laser, 31.01.2008, http://www.ringlaser.org.nz/content/g-0.php.

GFZ, 2008. SeedLink/SeisComP at the GFZ homepage http://www.gfz-potsdam.de/geofon/seiscomp/seedlink.html.

GSE, 1997. Provisional GSE 2.1 Messaage Formats & Protocols.

Huang, B.-S., 2003. Ground rotational motions of the 1999 Chi-Chi Taiwan earthquake as inferred from dense array observations. Geophys. Res. Lett. 30, 1307–1310.

Igel, H., Cochard, A., Wassermann, J., Flaws, A., Schreiber, U., Velikoseltsev, A., Dinh, N., 2007. Broad-band observations of earthquake-induced rotational ground motions. Geophysical Journal International 168 (1), 182–197.

Bibliography

Igel, H., Schreiber, U., Flaws, A., Schuberth, B., Velikoseltsev, A., Cochard, A., 2005. Rotational motions induced by the M8.1 Tokachi-oki earthquake, September 25, 2003. Geophys. Res. Lett. 32, L08309.

Johnson, C., Bittenbinder, A., Bogaert, B., Dietz, L., Kohler, W., 2008. Earthworm : A Flexible Approach to Seismic Network Processing, http://www.iris.iris.edu/newsletter/FallNewsletter/earthworm.html.

McLeod, D., Stedman, G., Webb, T., Schreiber, U., 1998. Comparison of standard and ring laser rotational seismograms. Geophysics Journal International 88, 1495–1503.

Moriya, T., Marumo, R., 1998. Design for rotation seismometers and their calibration. Geophys. Bull. Hokkaido Univ. 61, 99–106.

Nigbor, R., 1994. Six degree- of - freedom ground - motion measurements. BSSA 84, 1665–1669.

Orfeus, 2008. Software download portal http://www.orfeus-eu.org/Software/conversion.html.

Pancha, A., Webb, T., Stedman, G., McLeod, D., Schreiber, K., 2000. Ring laser detection of rotations from teleseimic waves. Geophysical Research Letters 27, 3553–3556.

Scherbaum, F., 1996. Of Poles and Zeros - Fundamentals of Digital Seismology. Kluwer Academic Publishers.

Schreiber, U., Igel, H., Cochard, A., Velikoseltsev, A., Flaws, A., Schuberth, B., Drewitz, W., Müller, F., 2005. The GEOsensor Project: a new observable for seismology. In: BMBF (Ed.), Geotechnologien. Springer Verlag.

Schreiber, U., Klügel, T., Stedman, G., 2003. Earth tide and tilt detection by a ring laser gyroscope. Journal of Geophysical Research 108, 2132.

Schreiber, U., Stedman, G., Igel, H., Flaws, A., 2006. Ring Laser Gyroscopes as Rotation Sensors for Seismic Wave Studies. In: Teisseyre/Takeo/Majewski (Ed.), Earthquake source asymmetry, structural media and rotation effects. Springer Verlag.

Solarz, L., Krajewski, Z., Jaroszewicz, L., 2004. Analysis of seismic rotations detected by two antiparallel seismometers: spline function approximation of rotation and displacement velocities. Acta Geophys. Pol 52, 197–217.

Spudich, P., Fletcher, J., 2008. Observation and prediction of dynamic ground strains, tilts and torsions caused by the M6.0 2004 Parkfield, California, earthquake and

aftershocks derived from UPSAR array observations. Bulletin of the Seismological Society of America .

Spudich, P., Steck, L., Hellweg, M., Fletcher, J.B., B. L., 1995. Transient stresses at Parkfield, California, produced by the M 7.4 Landers earthquake of June 28, 1992: Observations from the UPSAR dense seismograph array. J. Geophys. Res. 100, 675–690.

Stedman, G., 2001. Ring laser tests of fundamental physics and geophysics. Rev. Progr. Phys. 60, 615–688.

Stedman, G., Li, Z., Rowe, C., McGregor, A., Bilger, H., 1995. Harmonic analysis in a large ring laser with backscatter-induced pulling. Physical Review A 51, 4944–4958.

Suryanto, W., 2007. Rotational Motion in Seismology: Theory and Application. Ph.D. thesis, LMU Muenchen.

Suryanto, W., Wassermann, J., Igel, H., Cochard, A., Vollmer, D., Scherbaum, F., Velikoseltsev, A., Schreiber, U., dec 2006. First comparison of seismic array derived rotations with direct ring laser measurements of rotational ground motion. Bull. Seism. Soc. Am. 96 (6), 2059–2071.

Takeo, M., 1998. Ground rotational motions recorded in near-source region of earthquakes. Geophysical Research Letters 25, 789–792.

Takeo, M., Ito, H., 1997. What can be learned from rotational motions excited by earthquakes. Geophysical Journal International 129, 319–329.

Teisseyre, R., Suchcicki, J., Teisseyre, K., Wisznioswski, J., Palagio, P., 2003. Seismic rotation waves: basic elements of theory and recording. Annals. of Geophys. 46, 671–685.

UC, 2008. University of Canterbury, ring laser project website, 31.08.2008, http://www.phys.canterbury.ac.nz/research/laser.

UG-II, 2008. University of Canterbury, UG-II ring laser project, 31.01.2008, http://www.ringlaser.org.nz/content/ug-2_ultra_large_ring.php.

Velikoseltsev, A., Schreiber, K.-U., 2005. Observing earth from space - the GEOsensor Project. Tech. rep., Forschungseinrichtung Satellitengeodäsie der TU-München.

Wettzell, 2008. Fundamentalstation Wettzell homepage http://www.wettzell.ifag.de/.

Declaration

I hereby declare that this thesis has been written by myself and that I have only utilised resources as stated.

. . . .

Jan N. Hautmann
Munich, March 2008